



HAL
open science

Effect of cutting parameters on thrust force, torque, hole quality and dust generation during drilling of GLARE 2B laminates

Imed Boughdiri, Khaled Giasin, Tarek Mabrouki, Redouane Zitoune

► To cite this version:

Imed Boughdiri, Khaled Giasin, Tarek Mabrouki, Redouane Zitoune. Effect of cutting parameters on thrust force, torque, hole quality and dust generation during drilling of GLARE 2B laminates. *Composite Structures*, 2021, 261, pp.113562. 10.1016/j.compstruct.2021.113562 . hal-03327319

HAL Id: hal-03327319

<https://hal.science/hal-03327319>

Submitted on 13 Feb 2023

HAL is a multi-disciplinary open access archive for the deposit and dissemination of scientific research documents, whether they are published or not. The documents may come from teaching and research institutions in France or abroad, or from public or private research centers.

L'archive ouverte pluridisciplinaire **HAL**, est destinée au dépôt et à la diffusion de documents scientifiques de niveau recherche, publiés ou non, émanant des établissements d'enseignement et de recherche français ou étrangers, des laboratoires publics ou privés.



Distributed under a Creative Commons Attribution - NonCommercial 4.0 International License

Effect of cutting parameters on thrust force, torque, hole quality and dust generation during drilling of GLARE 2B laminates

Imed Boughdiri^{a,b}, Khaled Giasin^c, Tarek Mabrouki^a, Redouane Zitoune^b

^a Applied Mechanics and Engineering Laboratory (LR-11-ES19), University of Tunis El Manar, ENIT, BP 37, Le Belvédère, 1002 Tunis, Tunisia

^b Clément Ader Institute, UMR CNRS 5312, University of Toulouse, Toulouse, France.

^c School of Mechanical and Design Engineering University of Portsmouth. Portsmouth, UK

***Corresponding author:**

Redouane Zitoune: e-mail: redouane.zitoune@iut-tlse3.fr

Abstract

The present study investigates the effects of machining parameters and the tool coating during drilling of a GLARE[®] hybrid aerospace material on the cutting forces, hole quality and the generation of harmful dust particles. The drilling tests were conducted using twist drills with diamond-like carbon (DLC), Cristall coating and without coating. Obtained results indicate that feed, in contrast to spindle speed, has an important effect on thrust force and torque. In addition, when DLC coated tools are used less surface deviation was detected in comparison with uncoated and Cristall coated drills. Moreover, dust **measurement in terms of total number of particles, harmful particles and mass particles generated during drilling of GLARE[®] laminates was investigated. The results reveal that,** the number of harmful particles in the air was found to be dependent on machining parameters. In fact, a lower spindle speed promotes the reduction of the number of harmful particles in the air by 50 % compared to that observed at higher spindle speed.

Keywords:

GLARE[®]
Drilling
Twist drills
Drilling efforts
Hole quality
Drilling dust

1. Introduction

Increasing demand in the aerospace industry for high-performance and lightweight composites structures motivate a strong expanding development of fiber reinforced polymer composite laminates. Needs for improving material properties promote hybrid materials built-up from alternating metal layers (mostly aluminum alloy) and fiber reinforced composites [1]. Glass Aluminum Reinforced Epoxy (GLARE[®]) is a widely used fiber metal laminates (FMLs) in aerospace applications [2,3]. GLARE[®] is built-up from interlacing sheets of aluminum alloy Al2024 and R-glass or S-2 glass fiber layers bonded together using FM94 adhesive epoxy [4]. Panels, which are made of GLARE[®] are installed in the front and rear parts of the fuselage in Airbus A380 and they make a weight reduction of around 1000 kg in the fuselage and 90 kg in the vertical edges [3,5]. New challenges appear during the cutting of hybrid composite structures especially due to the large number of holes required with imposed quality criteria. For example, 750,000 holes are drilled in a single wing in Airbus A380 [4]. Add to this, poor hole quality causes a 60% rejection of parts [2]. Consequently, optimizing cutting conditions required for drilling FMLs with dissimilar materials will guarantee the imposed hole quality. Nevertheless, the poor surface finish may give rise to high stress on rivet joints and cause structure damages [6].

Machining of FMLs has been studied by few researchers, focusing on the effect of machining conditions and cutting tools on holes quality [7-9], thrust force, torque [10-12] and tool wear [13-15]. For machining multi-material composites, sharp and high hot hardness tool materials are required [8]. Poly-Crystalline Diamond (PCD), cemented carbide and high-speed steel (HSS) are the most common tool materials for machining FMLs. Coated carbide tools have better performance compared with uncoated tools in terms of tool wear at severe drilling conditions [6]. Pawar et al. [5] investigated the effect of tool size geometry on the evolution of thrust forces and hole quality of GLARE[®] and found that the two-flute drill is the best out of four different geometries used. This is thanks to the absence of delamination and less burr formation.

In another study by Mendes et al. [16], diamond-like carbon coated tools have been used to study cutting efficiency and it was found that they increased wear resistance and drill hardness. Krishnaraj et al. [11] reported that feed had a significant impact on the rise of thrust force when drilling CFRP/Al stacks.

Many experimental investigations had focused on measuring hole circularity error, cut surface roughness, burr formations and delamination during the drilling of composite/aluminum alloy stacks. The important parameters affecting hole quality are tool characteristics (drill grade, drill geometry) and machining parameters (feed, drilling speed, and cutting-fluid) [11]. Ashrafi et al. [6] found that AlTiN coated tools with finer surfaces reduced surface roughness by nearly 50% compared to that obtained using uncoated tools of the same geometry. Zitoune et al. [13] reported that drilling with a nano-composite coated drill (nc-CrAlN/a-Si₃N₄) remarkably reduces the cutting forces and the surface roughness of the holes drilled CFRP/Aluminum stack. Giasin et al. [17] investigated the impact of drilling parameters and tool coatings on surface roughness metrics (R_a and R_z) in GLARE[®] laminates. They found that R_a and R_z values of TiAlN coated tools were higher than TiN and AlTiN/TiAlN coated tools. They also found that R_a and R_z are proportional to spindle speed, but these metrics values change according to the coating types according to the variation of the feed.

In contrast, Zitoune et al. [7] mentioned, during hybrid composite metal stacks drilling, that arithmetic surface roughness R_a increases with the increase of feed, but spindle speed had a minor impact on surface roughness. Coesel [1] indicated that neither cutting parameters nor laminate thickness influenced the hole accuracy, in opposite with the result obtained by Tyczyski et al. [18]. Circularity and roundness are influenced by cutting speed and feed rate when drilling GLARE[®] with HSS and solid cemented carbide tools [19,20].

As known, the occurrence of the delamination phenomenon is also a challenge to overcome during the drilling of GLARE[®] and composites. For that, in order to suppress the drilling-induced delamination, Sorentino et al. [21] proposed an experimental technique based on

using variable feed rate. This technique is based on decreasing sharply the feed rate when the drill bit approaches the hole exit. Geng et al. [22] summarized that most delamination suppression strategies are drill design optimization and cutting conditions optimizations. For the optimization of tool design of twist drills which are the most used tools for drilling of aluminum/composites stacks, lower delamination is achieved with an angle point of 140° rather than 180° [23]. For the optimization of drilling conditions Geng et al. [22] reviewed different delamination suppression strategies, especially pre-drilled pilot holes, support plates and variable feed strategy. Giasin et al. [4] reported that the use of a backup plate at the exit side of a drilled hole in composites can minimize delamination and allow the suppression of crack growth when drilling composite materials. Nevertheless, when drilling GLARE[®], the aluminum sheets provide support to the glass fiber layers on both sides, which makes them resist peeling up and push out delamination. Shi et al. [24] studied delamination suppression when drilling of CFRPs. They deposited thermoplastic resin particle poly (polymethyl methacrylate) (PMMA), which induces less hole exit damage. In another work, Geng et al. [25] investigated Rotary Ultrasonic Elliptical Machining (RUEM) delamination suppression technique and found that RUEM technique improves significantly hole surface integrity and reduces delamination factor by 19.3% when compared to the technique consisting in varying tool feed rate. At the entrance and exit of the hole, the effect of cutting speed, feed rate and drill point angle on delamination was investigated by Bayraktar et al. [26] when drilling carbon fiber reinforced carbon matrix composites/Al 6013-T651 stacks with uncoated and coated drills. The optimization technique was based on Taguchi L9(33) orthogonal array experiment design. The analysis revealed that uncoated tools generated less delamination than the TiN and TiAlN coating tools and indicated that the optimal condition is obtained with a high cutting speed of 150 m/min, a low feed rate of 0.1 mm/rev and a drill point angle of 90° .

Also, during drilling composite-metal stacks and FMLs, the problem of chip formation must be studied since the evacuated chips rub continuously against the hole interior and may

cause poor surface finish. Additionally, the chips evacuated through the hole as well as the built-up edge at the cutting edges of the tool combined with increased tool wear can considerably affect the hole quality [7, 27] and can be responsible for the premature wear of the tool [28].

Most studies on metal stack composite machining focused on evaluating cutting mechanism and post-drilling measurements. Nevertheless, very few related studies focused on evaluating the emission of dust particles and the potential health hazards during the machining process [29-31]. Then, the knowledge around the nature of composite dust is still very limited. The quantity of dust generated during machining is influenced by factors such as material type and cutting parameters.

In this context, Djebara et al. [29] studied the impact of cutting parameters on small particle generation during aluminum alloys (6061-T6 and 7075-T6) machining. For this, a laser photometer (TSI8520 DusTrack™) was exploited to measure particle generation in the cutting area. The mentioned apparatus was connected to the dust recovery enclosure via a suction hose with a flow rate of 1.5 l/min. The authors mentioned that increasing cutting speed and feed reduced the emission of dust during machining. They explained that by the fragmentation of chips and high temperatures in the primary and secondary shear zones when machining with high cutting speeds and high feeds. It was found that ductile materials released more aerosols than brittle materials did [32]. As known, emitted particles have a significant bearing on health. So, it is necessary to find a method to reduce or control dust release without compromising hole quality. Some of these processes were MQL and dry machining used by Khettabi et al. [30] on milling of three types of aluminum alloys 7075, 6061 and 2024. The particle concentration was measured using a TSI instrument (particle scanning mobility particle sizer “SMPS”), which was connected to limbs of collection by a suction pipe. Then, the acquisition helps to analyze the particle concentration and the size distribution. Results show that the increase of flow rate lubrication of MQL increases particle generation, and dust size seems to increase at high cutting speeds.

For the evaluation of aerosols emission when machining of a composite material, Haddad et al. [31] used a dust monitor (portable aerosol spectrometer GRIMM, model 1.209) to measure the number of dust particles found in one liter of air and estimate its average size. The size of the dust particle range between 0.25 μm to 30 μm and they were measured every 6 s. The study reported that the small dust particles produced during the trimming of CFRP composite material at standard and high cutting speed seem to have a significant bearing on health. The small size of these particles that poses the hazard was superior for four flutes end mills in comparison with other geometries of coated and uncoated burr tools. Nguyen-Dinh et al. [33] investigated the effects of cutting parameters (feed speed and cutting speed), radial depth of cut and helix angle on the number of harmful particles during the trimming of CFRP specimens using the same dust monitor as [31]. Before beginning the measurements, an auto-test was carried out by passing particle-free filtered air into the closed chamber. Then, at least 3 measuring cycles of 6 s each were carried out to detect any existing particle contamination in the air. Results show that the number of harmful particles during trimming increased significantly with an increase in feed speed and a decrease in cutting speed. It was also observed that, when the radial depth of cut varies from 2 mm to 3 mm, a reduction in the number of harmful particles occurred. Kremer et al. [34] investigated the influence of the wear resistance on dust emission during machining metal matrix composite reinforced with several levels of SiC particles using PCD and CVD diamond tools. They used a GRIMM occupational dust monitors for particles calculation and size. The authors conclude that the percentage of reinforcement has different impacts on dust generation depending on the type of tool. For CVD tools, the major parameter is the wear rate: the amount of dust released increases with the level of reinforcement. On the other hand, dust emission with PCD tools is more sensitive to the tool chip interface, due to the better wear resistance of the drill. Bello [35] assessed airborne emissions during dry and wet abrasive cutting of two types of hybrid composites using two real-time particle sizers (FMPS Model 3091 and APS 3321). The first was a CFRP composite with aligned carbon nanotubes at the center layer

interface. The second was a fabric of alumina (Al_2O_3) fibers with aligned carbon nanotubes attached to the surface of the fibers, impregnated with an epoxy resin. Airborne exposure levels depend on the thickness and type of composite, while dust generation levels and concentrations of nanoparticles and fine particles are the same regardless of the presence or the absence of carbon nanotubes in hybrid composites. In another work, Bi [36] proposed the design of a system for controlling dust during the composite drilling process. The study modeled and simulated dust extraction system using the COSMOSFloWorks to be attached to the machine tool to guarantee a healthy environment for operators and achieve consistent quality of manufactured components. Iyer [37] used the same system developed by Jeffrey [38] to assess the effect of process variables on dust emissions (count of particles and dust concentration) during machining of Unidirectional CFRP composites and Random fiber HexMC[®] composites. He found that the count of particles increases with a decrease in feed rate and an increase in spindle speed and depth of cut. The concentration of particles is proportional to the depth of cut and inversely proportional to the feed rate, while spindle speed has little effect on the concentration. Despite having several studies on machining GLARE[®] laminates, nevertheless, none of the previous studies reported on dust generation during machining GLARE[®].

In this present study, uncoated and coated solid carbide (K20) drills with a diameter of 6 mm were used to drill holes in a GLARE[®] 2B 11/10-0.4 laminate. The main objective is to study the impact of machining parameters on cutting forces and torque evolutions. Besides, the specific cutting effort is exploited as an indicator to characterize the machinability of the work materials, quantitatively. Therefore, the assessment of hole quality includes the chip formation characterization and the measuring of both surface roughness and circularity error. These will help to identify optimized drilling conditions that guarantee the required hole quality and minimize thrust force and torque. Finally, the impact of the machining parameters as well as the tool coating on the dust generation was investigated.

2. Materials and experimental procedure

Different experimental setups were used to conduct drilling trials of GLARE[®] 2B 11/10 and to analyze hole surface quality.

2.1. Machine, workpiece and cutting tool details

Drilling tests were conducted on a DMU 85 mono BLOCK CNC milling machine with a maximum spindle speed of 18000 rpm. In this work, GLARE[®] 2B 11/10-0.4 was used as a workpiece material which composed of 11 sheets of aluminum alloy (with a nominal thickness of 0.4 mm) and 10 prepregs of S2-glass fibers embedded in an FM94 adhesive (with an approximate thickness of 0.133 mm) [4]. Mechanical properties of Al2024 alloy and S2/FM94 prepreg are shown in table 1 [2]. The lay-up sequence in each GFRP layer was [90°/90°] for GLARE[®] 2B, where the rolling direction in aluminum sheets is defined as (0°) as illustrated in Fig. 1(a). Table 2 depicts additional details of GLARE[®] 2B samples used in this experimental investigation [2].

The workpiece was cut into specimens with (205x19x7.13) mm³ in size by waterjet technology to facilitate the GLARE[®] mounting on the top of the dynamometer. The acquisition of cutting forces was carried out using a four-component Kistler dynamometer and Dynoware software (see Fig. 1(c) and (d)).

Coated and uncoated cemented carbide (grade K20) twist drills with 6 mm diameter were used when drilling GLARE[®] 2B 11/10-0.4 without coolant. This diameter is chosen according to the requirements of the aircraft industry [39], and the two types of coating are diamond-like carbon (DLC) and Cristall (diamond coating) (see Fig. 1(b)). All tools are manufactured by GUHRING[®].

DLC and Crystall possesses an outstanding hardness in excess of 8000 HV. These coatings are qualified for highly abrasive applications such as for example the machining of GFRP and CFRP, aluminium-alloys, ceramics and graphite. In the following, tools are labeled T1, T2, and T3 as mentioned in Table 3. Different spindle speeds and feeds, which were used for all experiments, are summarized in Table 4. Ten holes were drilled in each specimen with a new tool to avoid any effect that may be caused by the tool wear.

2.2. Measuring cutting forces

Cutting forces (F_z and M_z) during the machining process were measured using a piezoelectric Kistler 9272 dynamometer (Fig. 1(c)). During drilling processes, the dynamometer is connected to the charge amplifier (model 5019) in order to convert the piezoelectric signals to proportional electrical voltage signals. The sampling frequency was set to 3 KHz. The acquired data was processed by Dynaware software to present them in a force-time graph plot [Fig. 1(d)].

2.3. Measuring of surface roughness

Hole surface roughness has several effects on workpiece mechanical properties such as fatigue behavior, corrosion resistance, creep life, etc. Parameters characterizing surface quality roughness such as R_a , R_t and R_z can be used to assess defects on drilled hole surfaces. The 2D contact technique of measuring of the surface roughness is commonly used by industrial companies. The surface roughness profile was measured with a Mitutoyo SJ-500/P surface instrument with a sampling length of ($\lambda_c = 0.8$ mm, according to ISO 4288-1996) and an evaluation length of 6.4 mm. The number of sampling lengths was increased from the recommended value of 4 to 8 sampling lengths to account for the hybrid nature of GLARE® laminate. Calibration was performed before initiating roughness measurements using a Mitutoyo Precision reference specimen with a fixed R_a (see Fig. 2(a)). Fig. 2(b) represents the four roughness measurements that were made on each hole. The measurements of roughness profiles are recorded from each hole at four points. The measurements at point 1 and 2 were made in

such a way as to have the stylus parallel to the glass fibers (at 0° and 180°), the measurements at points 3 and 4 were made at 90° and 45°, respectively, for the orientation of the fibers.

2.4. Measuring of cylindricity and circularity error

Cylindricity and circularity measurements were performed using a Mitutoyo three dimensional CMM device with a ruby probe as shown in Fig. 2(c). Circularity was carried out by mapping eight points around the measured circle at a given depth, then calculating the difference between the greatest and the smallest radius measured from a certain central point of the circle, and finally tracing the perimeter of the cylinder with a probe. While the cylindricity was done by mapping eight locations around the hole with changing the depths: top at 1.825 mm, medium at 3.65 mm and bottom at 5.475 mm.

2.5. Measuring of dust

During drilling GLARE® 2B 11/10-0.4, small particles based on epoxy resin and glass qualified as the dust was generated. These particles have to be studied to highlight their significant bearing on the health that they seem to have. A dust monitor (portable aerosol spectrometer GRIMM, model 1.209) is used to measure the number of dust particles found in one liter of air during drilling of samples of GLARE® 2B – 11/10 (see Fig. 1(c)) **in a closed space with approximate dimensions of 1080 × 800 × 1500 mm³**. The results given by the spectrometer were an average of measurements for 6 seconds with a size of dust particles ranging between 0.25 µm to over 30 µm in 31 separate size channels in real-time, then the spectrometer supplies the calculated values as particle number and particle mass concentration.

Within the device, all particles are deposited on a PTFE filter of 47 mm diameter and can be used for gravimetric testing and further study. Within an optical measurement unit, every particle in the aerosol is measured independently through reflected light photometry. The dispersed light impulse of every individual particle is measured according to the intensity of the dispersed light signal corresponding to particle size. The aerosol spectrometer measures the

distribution of the particle scale of solid airborne particles in several levels of size. The device is calibrated using polystyrene spheres latex (PSL) [38]. During dust investigation, the number of particles has been read directly from the software (GRIMM). This software estimates the particle masses by considering only the density of air as a value of 1000 kg/m³. Also, particles are assumed to be spherical. When machining hybrid composite material, the particles are not spherical. Hence, their densities cannot be equal to 1000 kg/m³. This is precisely the reason that mass is calculated using the density of the composite material and particle shape is supposed cubic [31]. A disadvantage of the GRIMM 1.109 is that scanning 31 channels takes 6 seconds and needs longer samples compared to other real-time instruments that can scan at 1-second intervals.

3. Results and discussion

3.1. Thrust force and torque variations with spindle speed and feed

Fig. 3 represents a typical thrust force and torque measurement during a drilling cycle. Thrust force and torque profiles provide details about the beginning and the end of the drilling mechanism, the cutting progress and localization of drill bit at the metal-S2/FM94 composite interfaces. It can be underlined that the chisel edge starts to penetrate the first aluminum sheet, inducing a rapid increase in thrust force (F_z) and gradual increment of torque (M_z) (point 1). At point A, the drill reaches the first glass fiber/epoxy prepreg layer, where F_z and M_z values are less than those of point 1. **The reason behind this behavior is because of the difference in mechanical properties between the aluminum and glass fiber/epoxy.** At point 2, the chisel enters in contact with the second aluminum sheet, where the highest peaks in thrust force (F_z) and torque (M_z) were reached. Also, point B peaks of thrust force (F_z) and torque (M_z) were recorded for the S2/FM94 layer. So, it can be noted that thrust force (F_z) and torque (M_z) for drilling aluminum are always higher than S2/FM94 layers for used tools and with all different cutting conditions. For example, when using T1 at a feed of 0.12 mm/rev and spindle of 3000 rev/min maximum thrust forces are about 86 N and 167 N while torques are about 20 N.cm and 38 N.cm,

for GFRP and Al2024, respectively. As the tool penetrated through the alternating layers of aluminum and glass fiber, there is a significant change in the thrust force and torque variations. This analysis is in good agreement with those found in previous studies carried out when drilling hybrid materials with different tool geometry is used [2,7,40]. As the chisel advances through the workpiece, the cutting force (F_z) has a slight decrease due to lower work-piece resistance, whereas torque (M_z) has no clear change for both glass fiber layers and aluminum sheets. Finally, when the drill is completely out of the hole thrust forces and torque decrease rapidly to zero.

Fig. 4(a) shows the evolution of the thrust force (F_z) measured, during the drilling GLARE[®] 2B 11/10-0.4 with T1, T2 and T3 tools as a function of feed variations and a fixed spindle speed (3000rpm). Thrust force (F_z) increases as the feed increases from 0.02 mm/rev to 0.3 mm/rev for all tools. Thrust forces (F_z) recorded with Cristall coated tool T3 is 30-45% larger than those recorded during drilling with uncoated tool T1. For example, when drilling at 3000 rpm spindle speed and 0.3 mm/rev feed, it can be observed that for T3 the highest thrust force is about 294 N, whereas it is about 220 N for tool T1.

Fig. 4(b) shows the evolution of the thrust force (F_z) measured, during the drilling GLARE[®] 2B 11/10-0.4 with the same pre-cited tools as a function of spindle speed variations with a feed of 0.055 mm/rev. From the graph it can be observed that the thrust force remains approximately stable with spindle speed. This result is in agreement with previous studies on drilling composites alone or multi stacks [41].

For any condition tested, it was always found that T3 tools generate higher cutting forces compared to T1 and T2. This phenomenon can be explained by the fact that with T3, the web thickness is superior to T1 and T2 cutting tools. In fact, several studies have shown that increasing the web thickness from 0.6 to 1 mm increases the thrust force by 80% and the torque by 25% when drilling CFRPs with twist drills [42]. In addition, for coated tools, the coating layer presents a thermal barrier for the heat diffusion in the workpiece.

Fig. 4(c) shows the evolution of the torque force (M_z) when drilling with T1, T2, and T3 tools as a function of feed variations and a fixed spindle speed (3000 rpm). This torque increases as the feed increases from 0.02 mm/rev to 0.3 mm/rev for all tools. This is due to the increase in material removal rate when the feed is increased. Fig. 4(d) shows the evolution of the torque (M_z) with the same T3 tools regarding spindle speed variations with a fixed feed (0.055 mm/rev). Globally, three domains on the Fig. 4(d) can be underlined. During the first one (2000 to 4000 rpm), for each tool, there is a small increase in the torque with the increase of the spindle speed. It is speculated that the machining temperatures at this range of spindle speed does not cause significant effect on the mechanical properties of GLARE[®] constituents. In the second domain (6000 to 14000 rpm), torque (M_z) decreases with the increase of the spindle speed for all used tools. This phenomenon can be attributed to the high temperatures of machining due to the frictional phenomena. In fact, several authors have shown that the machining temperatures increase with the spindle speed and this softens the material constituents [43-45]. However, when the spindle speed is superior that 14000 rpm (third domain), a sudden increase in the torque is recorded. This can be attributed to the increased vibration of the cutting tool due to the dynamic effects of the machining process.

3.2. Analysis of specific cutting forces

Specific cutting force or said also specific cutting energy is defined by the following equation (1):

$$K_{c,f} = \frac{2.F_z}{d.f} \quad (1)$$

Where

- $K_{c,f}(N.mm^{-2})$: specific cutting force associated with the feed.
- F_z (N): average thrust force of Al2024 and S2/FM94.
- d (mm): diameter of the drill.
- f (mm/rev): feed.

This specific force corresponds to the energy required to remove one unit of material volume during the drilling operation. It is an indicator to evaluate quantitatively the machinability of the work materials by measuring cutting efficiency. So, the lower the specific energy, the lower is tool wear and the higher is the efficiency of the cut. Fig. 5(a) and (b) represents specific cutting force evolution regarding feed variation when drilling GLARE® 2B 11/10 with T1, T2, and T3.

The standard AFNOR (NF E 66-520) [46] defined several criteria for the optimal operating range of the machining conditions, among them:

- Specific cutting energy must decrease slightly or stabilize to optimize the tool lifetime.
- The cutting force evolution must be stable relative to the cutting force mean value.
- The machining quality must be in the chosen tolerances.

It was not possible to measure the thrust force of the two materials individually due to their small thicknesses. So, specific cutting force values reported in this study are calculated using a combination of both thrust forces measurements of aluminum sheets and S-2 glass fiber layers. The range corresponding to the first criterion (on stabilizing specific cutting energy) is easily identifiable especially for the holes drilled by the tools T1, T2, and T3. The optimum feed is about 0.055 mm/rev for the three tools used in drilling GLARE® 2B 11/4/10-0.4 (see Fig. 5(a) to (c)). However, the operating range is hardly identifiable for the spindle speed, as illustrated in Fig. 5(d); where specific cutting force evolution seems to be constant. The advantage of having optimal cutting conditions that minimize the specific cutting forces reduces tool wear. Unfortunately, no operating range can be deduced for the spindle speed based on specific cutting energy evolution in opposite to feed. Nevertheless, based on both thrust force and torque evolutions, it can be deduced that an optimal range of spindle speeds (corresponding to lower values of F_z and M_z) can be considered between 10000 and 14000 rpm.

As the machinability index of materials is evaluated by different parameters such as specific cutting force and surface finish, it is necessary to present in the next section the quality of drilled holes.

3.3. Analysis of drilled hole quality

3.3.1. Hole surface roughness

Hole surface roughness is taken as a criterion of qualification. Roughness measurements reported in this investigation are a combination of both roughness of aluminum sheets and S-2 glass fiber layers. It was not possible to measure the surface roughness of the two materials individually using the 2D surface profilometer due to their small thicknesses. Fig. 6(a) and (b) shows the evolution of average surface roughness R_a and total surface roughness R_t as functions of drill feed and spindle speed. It can be underlined that R_a and R_t increased with the rise of feeds. This is completely in agreement with the study of Giasin et al. [2]. Indeed, these authors found that surface roughness values increase with feed rate and spindle speed when drilling GLARE[®] 2B 11/10 or 8/7. The values of average surface roughness R_a were less than 3 μm in most drilled holes regardless of the type of tool. In the case of uncoated and coated drills, the total surface roughness R_t increases as the spindle speed increases from 2000 rev/min to 16000 rev/min when drilling GLARE[®] 2B 11/10 at a feed of 0.055 mm/rev. It was noticed that the maximum percentage of increases in R_t (45.125%) and R_a (49.12%) are observed for the tool T1. Also, the minimum percentage increases in R_t (5%) and R_a (7.8%) is for tool T3.

The maximum surface deviations were in drilled holes with uncoated tool T1 than that for DLC coated tool for different machining parameters as shown. This due to the better finished surface using coating tools which give a finer surface. This observation is in agreement with the results of Ashrafi et al.[6] and Giasin et al. [20].

From the Fig. 7, it can be observed that the surface roughness profile of the aluminum sheets is always lower than that of the glass fiber layers. The surface finish of the machined aluminum sheets, in general, can be said to be regular and smooth (lower difference between peaks and

valleys of the roughness profile), while the surface finish in the machined glass fiber layers is relatively fuzzier and irregular depending on the fiber's direction relative to the stylus path. For example, the bent fibers -due to the cutting process- tend to bounce back after the cutting-edge passes creating fuzziness and higher surface roughness [42]. In fact, Takeyama [47] mentioned previously that the roughness of the finished surface as a function of fiber orientation showed that the surface roughness rises significantly at a fiber orientation greater than 60° . The reason behind this is the presence of higher compressive stresses in the workpiece, which lead to higher surface roughness. It can be also concluded that fiber orientation affects the microstructure of the machined surface [48, 49]. This is can be explained by the inhomogeneity of the glass fiber layers in the laminate and the effect of fiber orientation relative to the direction of cut [49, 50]. The technique used here for the qualification of the machining surface is affected by the process of the cutting of the composite (fiber size, porosity, fuzziness of the fibers). In this configuration of measurement, the stylus of the roughness tester might get entangled by the fibers which can lead to errors in the final results of the measurements [50]. In another work on drilling GLARE®, a 3D optical profilometer was used to characterize the quality of the holes, it was found that the relative position of the fibers with respect to the stylus head influences the roughness value [4].

Fig. 8 (a) and (b) shows R_z values measured at positions of 0° , 45° , 90° and 180° in GLARE® 2B 11/10 drilled with all tools at different feeds and spindle speed. Roughness R_z values measured at 45° and 90° are higher than those measured at 0° and 180° for the same hole (>96% of the total drilled holes). This marks the influence of the direction of measurement for the fiber orientation on the surface roughness. This observation is in accord with the findings of Eneyew et al. [51] and Li et al. [52]. In addition, similar results are obtained by Cadorin et al. [60], when drilling of 3D woven composite with and without coolant. Generally, R_z of holes drilled with the three types of cutting tools increases with spindle speed and decreases with feeds. This trend of R_z variation versus spindle speed is the same for R_a and R_t for all used tools. The highest value of R_z

roughness measurement was recorded when the stylus was at a 45° position. Random values of R_z values were observed during GLARE® 2B 11/10 drilling. This can be explained as mentioned by Giasin et al. [20] to the fibrous and brittle nature of glass fibers. For the impact of coating on R_z roughness, it can be underlined from Fig. 8 (a) and (b) that DLC coated tool T2 presents better results in comparison with uncoated tool T1 and Cristall coated tool T3. Also, it was noticed that the difference between R_z values and R_t values under different cutting conditions is important regardless of the type of tool coating. Therefore, when measuring the surface roughness in the laminate at the four locations described previously, there will be a variation in the surface roughness depending on the contact between the fibers and the tip of the stylus around the hole. A more realistic and robust evaluation of roughness metrics in GLARE® laminates would be to evaluate the roughness of its constituents (i.e. the glass fiber layers and the aluminum sheets) separately by extracting average roughness data from the roughness profile for each of the materials. This evaluation will be considered in a future study.

As a conclusion for surface roughness assessment, the investigation of hole surface roughness (R_a , R_t , and R_z) in terms of feed and spindle speed shows that fewer surface defects are obtained when drilling GLARE® 2B 11/10 -0.4 samples with lower spindle speed and feed as mentioned in the previous study of Giasin et al. [20]. It can be underlined also that DLC coating leads to a better hole surface roughness in comparison with Cristall coated tool and uncoated tool. In addition, the current results of arithmetic roughness R_a were within the surface roughness range of those reported by Giasin et al. [20]. The range of surface roughness values is from 1.16 to 2.13 μm of the under-tested cutting parameters. As mentioned in the literature, there is no available data indicating the required surface roughness for GLARE® materials or metal-stacked composite materials for the machining/drilling application in the aerospace industry. Manufacturers and cutting tool specialists such as Sandvik [53] have reported that the most common aerospace manufacturing requirements with respect to hole surface quality for R_a do not

exceed $3.2\ \mu\text{m}$ for CFRP and $1.6\ \mu\text{m}$ for Al or Ti, and this is the case for almost all of the roughness values found in the present investigation.

3.3.2. *Cylindricity and circularity error*

Fig.9 shows circularity errors of holes when drilled with coated and uncoated tools versus different feeds and spindle speeds. Results revealed that increasing feed does not influence the circularity of drilled holes when using T1 whereas the variation of the precited errors can be detected for tools T2 and T3. It can be also observed that holes drilled using coated tools (T2 and T3) produced less deviation and error than the uncoated tool (T1) (see Fig. 9(a)). This can be explained by the fact that coated tools with the finer layer induce drilled holes which approximate to a true circle [6]. Circularity errors tend to increase with increasing spindle speed from 2000 rpm to 18000 rpm (see Fig. 9(b)). This was most likely due to the instability of the cutting tool which induced vibrations and higher distortions [4].

Fig. 10(a) to (f) presented cylindricity of drilled holes at the top, the medium and bottom locations under different cutting conditions using the three tools T1, T2, and T3. The cylindricity was found higher, for both coated and uncoated tools at the first depth (1.825 mm) at different machining parameters. The reason attributes to the fact that hard metal chips evacuated through the entry of the hole, producing a rougher surface than the exit of the hole (depth of 5.745 mm) as reported by Ashrafi et al. [6] when drilling CFRP/AL/CFRP stacks. In general, deviations in circularity errors were up to $33\ \mu\text{m}$. The geometrical discrepancies observed, however, were not considered excessive according to industrial requirements and could be considered to be acceptable with a reaming operation following drilling [9].

Fig.11 shows cylindricity for T1, T2, and T3 versus feeds and spindle speeds. In general, deviations in cylindricity were up to 0.0389 mm, 0.0339 mm and 0.0588 mm for the T1, T2 and T3 at a spindle speed of 3000 rpm, respectively (see Fig. 11(a)), while cylindricity at fixed feed varied between 0.0119 mm and 0.0274 mm (see Fig. 11(b)). The geometrical discrepancies

found when drilling of GLARE® 2B 11/10, were not considered excessive according to industrial requirements.

As a conclusion, cylindricity deviations during dry drilling of GLARE® 2B 11/10 laminates were up to 0.06 mm, while circularity error over the entire stack varied between 0.004 mm and 0.035 mm. In general, smaller deviations in cylindricity and circularity error is required and since there was no specific reference standard for hole deviations. Through the comparison with results from previous literature reported by Giasin et al. [4], cylindricity and circularity deviations found in this investigation are not considered excessive in relation to industrial requirements.

3.3.3. Chip formation analysis

At the microscale analysis, two types of chip were observed during drilling for any condition of drilling tested or type of tool used. The first type has powder form which is commonly observed when machining composites. The size of the formed powder depends on the cutting mechanism which is strongly influenced by the relative angle between the direction of the fiber and the direction of the cutting speed, as well as the machining parameters used (Feed, speed) [33]. In addition, the powdery glass fiber chips can be related to the brittle fracture phenomenon which is usually observed when machining composites made from thermoset materials [42]. The second type of chips have a continuous form which characterizes the cutting process in metallic materials such as aluminum and titanium. During machining of multilayers acceptable metal chips can be evacuated without damaging the internal hole wall. In machining metallic alloys, continuous chips are preferred over broken chip because continuous chips can result in smooth surface finish. However, when machining multi material stacks, the evacuated continuous metal chips from the hole can increase the roughness of the composite layers. In this case, the interaction between the continuous chip and the composite layers favors the degradation of the matrix and the fiber due to the erosion phenomena (such as collision of sharp chips with the composite layers). This phenomenon is more pronounced when the feed is less or

equal to 0.08 mm/rev as entangled chip is seen to form at this feed, this form of chips is observed for any cutting tool or spindle speed used (see Fig.12). This in return would result in increasing of the roughness of the wall of the hole. However, when drilling is conducted using a feed of 0.2 mm/rev or higher, no entangled chip is observed which favors the increase of the roughness. This can be explained by the fact that when increasing the feed rate, the chip thickness increase which helps the formation of shorter chips compared to when drilling using lower feed rates [54]. In fact, a thicker uncut chip requires higher cutting forces due to the increase in the volume of the material removed from the workpiece [55].

Therefore, after every drilled hole of GLARE[®] 2B 11/10-0.4, only chips formed from aluminum sheets were collected for analysis. These chips indicate that the chip thickness and length increased with the increase of the feed. An ISO-based chip form classification chart is used for quantitative evaluation of the size and shape of the chips being produced from the drilling tests [56]. For T1 and T2, long helical chips were formed at low feed and spindle speed, while snarled helical chips and snarled corkscrew chips with minimal curling were formed at higher feed and spindle speeds of 0.25 mm/rev and 16000 rpm (Fig.12).

For T2, when drilling at low feed of 0.04 mm/rev the chip demonstrates an overlapping geometry and tended to wrap (entangle) around the cutting tool. In some cases, after every drilling operation, it was observed that some of the aluminum chips tended to entangle around the cutting tool body which required removing them manually after the drilling of each hole. This can cause some problems during automatic drilling and riveting of composites structures. Indeed, in addition to downtime, which can generate additional costs, the machined holes can be damaged by overlapped chips and adhered to the active part of the tool [13].

The chips formed from T1 and T2 at higher feeds are shorter, tended to easily evacuation from the cutting zone and did not curl around the drilling bit, as shown in Fig. 11. This reveals that a compromise between spindle speed and feed is required to achieve a better hole quality and reduce the machining time [49]. Long helical chips as shown in T1, T2 (0.04 mm/rev and 0.08

mm/rev) are not ideal in terms of both chip evacuation and surface finish of the drilled hole [54]. Chip formation in T1, T2 (0.2 and 0.25 mm/rev) holes are ideal as the chip formed here is short spiral and snarled one which is easier to evacuate.

3.4. Dust measurements

3.4.1. Number of particles

When machining composites such as GLARE[®], the cutting process is the result of the aluminum sheet failure and the fracture of the S2/FM94 layer which induces the formation of a fragmented powdery chip with micrometric size [31].

As mentioned before, the GRIMM 1.109 Portable Aerosol Spectrometer measures the number of particles present in one liter of air in sizes ranging from 0.25 μm to 32 μm in 31 different size channels. To have clear and consistent data and better understand the effect of the cutting parameters, the particle sizes considered are reduced to 6 ranges. These ranges are chosen to reflect the different peaks: between 0,25 μm and 1 μm , between 1 μm and 2 μm , between 2 μm and 3 μm , between 3 μm and 4 μm , between 4 μm and 5 μm , and finally particles larger than 5 μm . For example, the number of particles in the size range (0.25 μm to 1 μm) is calculated as follows:

$$N_{[0.25-1\mu\text{m}]} = N_{[0.25-0.28\mu\text{m}]} + N_{[0.3-0.35\mu\text{m}]} + \dots + N_{[0.8-1\mu\text{m}]} \quad (2)$$

Fig.13 represents the number of particles of different sizes present in one liter of air for different cutting conditions and the three tools T1, T2, and T3. It is noted that most of the particles present in the air have sizes between 0.25 μm and 1 μm . In other studies, most particles generated are of a size ranging from 0.5 μm to 1.5 μm when drilling hybrid bio-composite material [52] and from 0.25 μm to 0.7 μm when trimming CFRP composite material [33]. Another less pronounced range of particles can be found between 1 μm and 2 μm , showing a smaller number of particles than the first range. The other ranges have very low particle numbers. It is important to mention that, for all the uncoated and coated tools, the number of

particles in the size range (0.25 μm to 1 μm) corresponds to the major percentage measured and represents more than 96 % of the total number of particles. Fig. 13(a) to (c) indicated that the increase in the feed induces a decrease in the number of particles for each size range. Moreover, an increase in cutting speed induces an increase in the number of particles for each size range when using the three drills.

Fig. 14(a) and (b) present the variation of the total particle number measured versus (a) feeds (b) spindle speeds. It was seen that the highest total number of particles per air liter is obtained for the spindle speed of 18000 rev/min and a feed of 0.055 mm/rev. These values correspond to the highest cutting speed and the optimum feed. Generally, a decrease in the feed from 0.25 mm/rev to 0.02 mm/rev and an increase in spindle speed from 2000 rpm to 18000 rpm induced the rise in the total number of particles present in 1 liter when drilling GLARE[®] 2B 11/10-0.4 with tools T1, T2 and T3. This can be explained by the fact that the theoretical chip thickness is proportional to the feed and inversely proportional to the spindle speed, therefore the theoretical chip size increases with the feed and decreases with increasing spindle speed. This invariably leads to a decrease in the number of dust particles present in the air. Indeed, the finer the chips have become, the finer dust is generated by their defragmentation. Moreover, when the dust is fine, it will be present in large numbers in suspension in the air (due to its very low weight). In the same way, from certain sizes upwards, these dusts fall under the effect of their weight [57].

Results obtained with both types of tools can't help us to make a comparison between coated and uncoated tools in terms of particle number. Therefore, drill coatings have different influences on the number and size of particles in the air when compared to uncoated drills. These observations are not totally in agreement with the results found by Haddad et al. [31] during the analysis of dust generated while trimming CFRP composites. It appears that DLC coated tool T2 can induce a minimum total particle number than uncoated tool T2 and Cristal coated tool T3. Moreover, T1 ensures less dust generation than coated tool T3. Cristall coating is characterized by a single-

layer structure So its micro-crystalline morphology presents small asperities, which generate a less protective layer and a rough contact that increases particle generation.

3.4.2. Mass of particles

The size and number of particles are not enough to indicate the hygienic and safe measures to adopt when machining GLARE[®] 2B 11/10-0.4 composites stacks. Indeed, knowing that the majority of these particles have sizes less than 1 micron, no conclusion can be made from the number alone.

A dust monitor (portable aerosol spectrometer GRIMM, model 1.209) is used to measure the mass of dust particles found in one liter of air during drilling of samples of GLARE[®] 2B – 11/10 (see Fig. 1(c)). The results given by the spectrometer were an average of measurements for 6 seconds with a size of dust particles ranging between 0.25 µm to over 30 µm.

The total mass of particles is calculated for different machining parameters by multiplying only the density of the S2 Glass/FM 94 Epoxy prepreg material (1980 kg/m³) by the volume generated by the sum of the volume formed by different particles. It is therefore proposed to match the number of particles to their respective weights by assuming that each particle is a cube. It can be underlined here that each cube has a characteristic side equals to the mean value of each interval (for example range 0.25-0.28 µm; a = 0.265 µm).

Consequently the mass for dust particles as calculated as following [31]:

$$Mass = \rho \times (0.265^3 \times N_{[0.25-0.28]} + 0.325^3 \times N_{[0.3-0.35]} + \dots + 0.675^3 \times N_{[6.5-7.5]} + \dots + 11.25^3 \times N_{[>32 \mu m]}) \quad (3)$$

From equation (2), the results obtained are grouped and drawn in Fig. 15(a) and (b).

Exposure limits values are defined in the labor code (article R4222-10). In rooms with specific pollution, the average concentrations of total and alveolar dust in the atmosphere inhaled by a worker, evaluated over a period of eight hours, must not exceed 10 and 5 mg/m³ of air respectively [58]. Occupational Safety and Health Administration agency in the USA and the Labor Safety and Health Act (JAPAN) defined the carbon fiber exposure limit (ppm). These

values are 2 and 2.9 mg/m³ respectively in terms of total dust in the air evaluated over 8 hours [59].

In the present research work, dust generated during drilling GLARE[®] as a function of feed never exceeds the limit exposure values (see Fig. 15 (a)). Fig. 15(b) represents the variation of total particles masses present in 1 L of air as a function of spindle speed. It can be seen that the total mass of the particles is less than total and alveolar dust values defined by [58], but the dust values obtained are significantly higher than the carbon fiber exposure limit (ppm) [59] regardless of the type of used tools (uncoated and coated). This can be related to decreasing in chip thickness. Indeed, the chip thickness decreases as spindle speed rise as reported previously. So, drilling with higher spindle speed induces small chips; hence a great number of small size chips are easily generated in the air because of their lighter weight [33].

As reported by Haddad et al. [31] the most harmful particles are therefore those reaching the pulmonary alveoli (Zone 1) and sizing between 0 and 10 microns. Consequently, it is necessary to study the mass of the harmful particles which can be formulated by the following equation (4) [31]:

$$\text{Masse} = \rho * (0.265^3 * A + 0.325^3 * B + 0.425^3 * C + 0.54^3 * D + \dots + 45^3 * J + \dots + 9.25^3 * L + \dots + 32^3 * M) \quad (4)$$

Where the constants A, B, C, D ...M, are detailed in table 5.

From this formula, it can be assumed that the composite fibers are attached to the resin. The evolution of dangerous particle mass at different cutting conditions is illustrated in (see Fig. 15(c) and (d)).

The mass of minimum harmful particles is obtained by the uncoated tool for the lowest spindle speed and the optimum feed. However, the tool T1 has recorded a bigger value for mass, at constant spindle speed and with a feed of 0.02 mm/rev (see Fig. 15(c) and (d)). Generally, during drilling GLARE[®], harmful particles masses don't exceed the limit exposure values, defined by [58] and [59] when the feed rate increases from 0.02 mm/rev to 0.25 mm/rev and spindle speed increases from 2000 rpm to 16000 rpm. This can be explained by the superior

density of GFRP (1980 kg/m³) compared to the density of CFRP (1580 kg/m³). Then, the particles of dust generated will tend to fall under the effect of its weight. Further, the health hazard which is directly related to the dust generated is less when using the GFRP structure instead of CFRP. So, machining of hybrid composite material based on glass fiber seems to have fewer health hazards than CFRP.

Also, other precautions should be taken, and it is strongly recommended that a vacuum system, suitable masks, gloves, and lab coats must be used during the machining of composite materials. Inhalation can be prevented by avoiding hand-to-mouth contact and peri-oral route, restricting consumables and consumption (food, drink, gum, tobacco), and regularly washing hands after any operation including composite material, even when gloves are worn [59].

4. Conclusion

In this paper, an experimental study of the drilling of GLARE[®] 2B 11/10-0.4 stack, using uncoated and coated tools (DLC coated tool and Cristall coated tool), was conducted at various cutting conditions. The influence of machining parameters (feed and spindle speed) on the drilling process was evaluated in terms of thrust force, torque, specific cutting force, hole surface quality, cylindricity, and circularity errors. The following conclusions can be drawn:

- The feed rate is the main cutting parameter affecting the cutting forces (thrust force and torque). When the feed is varied from 0.02 to 0.3 mm/rev, the thrust force and the torque increased by 80% and 85%, respectively. However, when the spindle speed varied from 2000 to 18000 rpm, the thrust force remains approximately stable (around 2% reduction). In addition, the torque increased when varying the spindle speed from 2000 to 6000 rpm and decreased when the spindle speed was varied from 6000 to 14000 rpm. This phenomenon can be attributed to the increased machining temperatures at high spindle speeds. This in return increased the softening of GLARE[®] constituents especially in the metallic material. Finally, at high spindle speeds (superior to 14000 rpm), a sudden

increase in the thrust force was observed due to the increased vibrations during the machining process.

- As qualitative results, it was observed that specific cutting efforts decrease slightly or remain stable for the three tools used for an optimum feed equals to 0.055 mm/rev.
- It can be concluded that the surface roughness values are significantly affected by the position of measurement. In fact, it was observed that the small value of the roughness is recorded at positions 0 and 180 degrees were small compared to the roughness values measured at 45 and 90 degrees.
- Increasing feed does not influence the circularity of drilled holes, this may be due to the effect of the tip geometry of the drills, whereas circularity error measurements tend to increase with increasing spindle speed.
- Different shapes and sizes of chips were formed at different cutting conditions when drilling of GLARE® 2B 11/10-0.4 stack, using uncoated and coated tools, the chip thickness increases with feed increase and spindle speed decrease.
- Dust generation becomes an important indicator for machining performance and has to be considered for safety health operators. The quantity of dust generated during machining is influenced by factors such as material type and cutting parameters.
- The main parameters affecting the number and the mass of harmful particles are the cutting parameters and tool coatings. The increase in feed rate and the decrease in spindle speed induce a reduction in the number of harmful particles in the air.
- The highest number of particles was obtained for the highest spindle speed of 18000 rpm. The mass of minimum harmful particles was recorded for the uncoated tool at lower spindle speed and optimum feed. Also, drilling GLARE® 2B 11/10-0.4 stack with lower spindle speed will generate a smaller number of harmful particles.

- Optimization of cutting parameters provides a better surface quality and less harmful dust generation is required when drilling GLARE® 2B 11/10-0.4 stack.

Acknowledgments

This project was realized in Clément Ader Institute (Paul Sabatier University of Toulouse 3) and MAI laboratory (University of Tunis El Manar, ENIT, Tunis, Tunisia). The authors wish to thank Xavier Sourd, Abdellah Bouzid and Akshay Hejjejj from Clément Ader Institute for their technical support. The authors would also like to thank the Fiber Metal Laminate center in the Netherlands and Prof. Jos Sinke for the provision of GLARE® sample. The authors would also like to thank Guhring® cutting tools company and Mr. Ian Goffey for the kind support of providing the cutting tools.

References

- [1] Coesel JFW. Drilling of fibre-metal laminates. 1994.
- [2] Giasin K, Ayvar-Soberanis S, Hodzic A. An experimental study on drilling of unidirectional GLARE fibre metal laminates. *Compos Struct* 2015;133:794–808. <https://doi.org/10.1016/j.compstruct.2015.08.007>.
- [3] Sinmazçelik T, Avcu E, Bora MÖ, Çoban O. A review: Fibre metal laminates, background, bonding types and applied test methods. *Mater Des* 2011;32:3671–85. <https://doi.org/10.1016/j.matdes.2011.03.011>.
- [4] Giasin Khaled, Ayvar-Soberanis Sabino. An Investigation of burrs, chip formation, hole size, circularity and delamination during drilling operation of GLARE using ANOVA. *Compos Struct* 2017;159:745–60. <https://doi.org/10.1016/j.compstruct.2016.10.015>.
- [5] Pawar OA, Gaikhe YS, Tewari A, Sundaram R, Joshi SS. Analysis of hole quality in drilling GLARE fiber metal laminates. *Compos Struct* 2015;123:350–65. <https://doi.org/10.1016/j.compstruct.2014.12.056>.
- [6] Ashrafi S a., Sharif S, Farid a. a., Yahya M. Performance evaluation of carbide tools in drilling CFRP-Al stacks. *J Compos Mater* 2013;48:2071–84. <https://doi.org/10.1177/0021998313494429>.
- [7] Zitoune R, Krishnaraj V, Collombet F. Study of drilling of composite material and aluminium stack. *Compos Struct* 2010;92:1246–55. <https://doi.org/10.1016/j.compstruct.2009.10.010>.
- [8] Kuo CL, Soo SL, Aspinwall DK, Thomas W, Bradley S, Pearson D, et al. The effect of cutting speed and feed rate on hole surface integrity in single-shot drilling of metallic-composite stacks. *Procedia CIRP* 2014;13:405–10. <https://doi.org/10.1016/j.procir.2014.04.069>.
- [9] Shyha IS, Soo SL, Aspinwall DK, Bradley S, Perry R, Harden P, et al. Hole quality assessment following drilling of metallic-composite stacks. *Int J Mach Tools Manuf* 2011;51:569–78. <https://doi.org/10.1016/j.ijmachtools.2011.04.007>.

- [10] Giasin K. The effect of drilling parameters , cooling technology , and fiber orientation on hole perpendicularity error in fiber metal laminates. *Int J Adv Manuf Technol* 2018;97:4081–99.
- [11] Krishnaraj V, Zitoune R, Collombet F, Davim JP. Challenges in Drilling of Multi-Materials. *Mater Sci Forum* 2013;763:145–68. <https://doi.org/10.4028/www.scientific.net/MSF.763.145>.
- [12] Wang CY, Chen YH, An QL, Cai XJ, Ming WW, Chen M. Drilling temperature and hole quality in drilling of CFRP/aluminum stacks using diamond coated drill. *Int J Precis Eng Manuf* 2015;16:1689–97. <https://doi.org/10.1007/s12541-015-0222-y>.
- [13] Zitoune R, Krishnaraj V, Sofiane Almabouacif B, Collombet F, Sima M, Jolin A. Influence of machining parameters and new nano-coated tool on drilling performance of CFRP/Aluminium sandwich. *Compos Part B Eng* 2012;43:1480–8. <https://doi.org/10.1016/j.compositesb.2011.08.054>.
- [14] Kuo CL, Soo SL, Aspinwall DK, Bradley S, Thomas W, M'Saoubi R, et al. Tool wear and hole quality when single-shot drilling of metallic-composite stacks with diamond-coated tools. *Proc Inst Mech Eng Part B J Eng Manuf* 2014;228:1314–22. <https://doi.org/10.1177/0954405413517388>.
- [15] Carrilero MS, Alvarez M, Ares JE, Astorga JR, Cano MJ, Marcos M. Dry drilling of Fiber Metal Laminates CF / AA2024 . A preliminary study. *Mater Sci Forum* 2006;526:73–8. <https://doi.org/10.4028/www.scientific.net/MSF.526.73>.
- [16] Batista Mendes GC, Padovan LEM, Ribeiro-Júnior PD, Sartori EM, Valgas L, Claudino M. Influence of implant drill materials on wear, deformation, and roughness after repeated drilling and sterilization. *Implant Dent* 2014;23:188–94. <https://doi.org/10.1097/ID.0000000000000028>.
- [17] Giasin K, Gorey G, Byrne C, Sinke J, Brousseau E. Effect of machining parameters and cutting tool coating on hole quality in dry drilling of fibre metal laminates. *Compos Struct* 2019;212:159–74. <https://doi.org/10.1016/j.compstruct.2019.01.023>.
- [18] Tyczyski P, Lemaczyk J, Ostrowski R, Sliwa RE. Drilling of CFRP, GFRP, glare type composites. *Aircr Eng Aerosp Technol An Int J* 2014;86:312–322. <https://doi.org/10.1108/AEAT-10-2012-0196>.
- [19] Park SY, Choi WJ, Choi CH, Choi HS. Effect of drilling parameters on hole quality and delamination of hybrid GLARE laminate. *Compos Struct* 2017;185:684–98. <https://doi.org/10.1016/j.compstruct.2017.11.073>.
- [20] Giasin K, Ayvar-Soberanis S, Hodzic A. The effects of minimum quantity lubrication and cryogenic liquid nitrogen cooling on drilled hole quality in GLARE fibre metal laminates. *Mater Des* 2016;89:996–1006. <https://doi.org/10.1016/j.matdes.2015.10.049>.
- [21] Sorrentino L, Turchetta S, Bellini C. A new method to reduce delaminations during drilling of FRP laminates by feed rate control. *Compos Struct* 2018;186:154–64. <https://doi.org/10.1016/j.compstruct.2017.12.005>.
- [22] Geng D, Liu Y, Shao Z, Lu Z, Cai J, Li X, et al. Delamination formation , evaluation and suppression during drilling of composite laminates: A review. *Compos Struct* 2019;216:168–86. <https://doi.org/10.1016/j.compstruct.2019.02.099>.
- [23] Shyha I, Soo SL, Aspinwall D, Bradley S. Effect of laminate configuration and feed rate on cutting performance when drilling holes in carbon fibre reinforced plastic composites. *J*

- [24] Shi Y, Wang X, Wang F, Gu T, Xie P, Jia Y. Effects of inkjet printed toughener on delamination suppression in drilling of carbon fibre reinforced plastics (CFRPs). *Compos Struct* 2020;245:112339. <https://doi.org/10.1016/j.compstruct.2020.112339>.
- [25] Geng D, Liu Y, Shao Z, Zhang M, Jiang X. Delamination formation and suppression during rotary ultrasonic elliptical machining of CFRP. *Compos Part B* 2020;183:107698. <https://doi.org/10.1016/j.compositesb.2019.107698>.
- [26] Bayraktar S, Turgut Y. Determination of delamination in drilling of carbon fiber reinforced carbon matrix composites / Al 6013-T651 stacks. *Measurement* 2020;154. <https://doi.org/10.1016/j.measurement.2020.107493>.
- [27] E. Brinksmeier RJ. Drilling of Multi-Layer Composite Materials consisting of Carbon Fiber Reinforced Plastics (CFRP), Titanium and Aluminum Alloys. *CIRP Ann* 2002;51:87–90.
- [28] Zitoune R, Krishnaraj V, Collombet F, Le Roux S. Experimental and numerical analysis on drilling of carbon fibre reinforced plastic and aluminium stacks. *Compos Struct* 2016;146:148–58. <https://doi.org/10.1016/j.compstruct.2016.02.084>.
- [29] Djebara A, Jomaa W, Bahloul A, Songmene V. Dust emission during dry machining of Aeronautic Aluminum Alloys +. *Proc 1st Int Conf Aeronaut Sci*, 2013, p. 1–8.
- [30] Khettabi R, Zedan Y. On particle emission during machining of titanium and aluminum alloys. *CIRP J Manuf Sci Technol* 2013;6:175–80. <https://doi.org/https://doi.org/10.1016/j.cirpj.2013.04.001>.
- [31] Haddad M, Zitoune R, Eyma F, Castanie B. Study of the surface defects and dust generated during trimming of CFRP: Influence of tool geometry, machining parameters and cutting speed range. *Compos Part A Appl Sci Manuf* 2014;66:142–54. <https://doi.org/10.1016/j.compositesa.2014.07.005>.
- [32] Balout B, Songmene V, Masounave J, Engineering M, De É. An Experimental Study of Dust Generation During Dry Drilling of Pre-Cooled and Pre-Heated Workpiece Materials. *J Manuf Process* 2007;9:23–34.
- [33] Nguyen-Dinh N, Hejjaji A, Zitoune R, Bouvet C, Salem M. New tool for reduction of harmful particulate dispersion and to improve machining quality when trimming carbon/epoxy composites. *Compos Part A Appl Sci Manuf* 2020;131:105806. <https://doi.org/10.1016/j.compositesa.2020.105806>.
- [34] Kremer A, El Mansori M. Tool wear as-modified by particle generation in dry machining. *Wear* 2011;271:2448–53. <https://doi.org/10.1016/j.wear.2010.12.030>.
- [35] Bello D, Wardle BL, Yamamoto N, Guzman DeVilloria R, Garcia EJ, Hart AJ, et al. Exposure to nanoscale particles and fibers during machining of hybrid advanced composites containing carbon nanotubes. *J Nanoparticle Res* 2009;11:231–49. <https://doi.org/10.1007/s11051-008-9499-4>.
- [36] Bi Z. Design and simulation of dust extraction for composite drilling. *Int J Adv Manuf Technol* 2010;54:629–38. <https://doi.org/10.1007/s00170-010-2971-1>.
- [37] Iyer AK. Characterization of Composite Dust generated during Milling of Uni-Directional and Random fiber composites. 2015.

- [38] Miller JL. Investigation of Machinability and Dust Emissions in Edge Trimming of Laminated Carbon Fiber Composites. 2014.
- [39] Giasin K, Ayvar-Soberanis S, Hodzic A. Evaluation of cryogenic cooling and minimum quantity lubrication effects on machining GLARE laminates using design of experiments. *J Clean Prod* 2016;135:533–48. <https://doi.org/10.1016/j.jclepro.2016.06.098>.
- [40] Shyha I, Soo SL, Aspinwall DK, Bradley S, Dawson S, Pretorius CJ. Drilling of Titanium/CFRP/Aluminium Stacks. *Key Eng Mater* 2010;447–448:624–33. <https://doi.org/10.4028/www.scientific.net/KEM.447-448.624>.
- [41] Karimi NZ, Minak G, Kianfar P, Heidary H. The Effect of Chisel Edge on Drilling-Induced Delamination. *18th Int Conf Compos Struct*, vol. 3, 2016, p. 36250.
- [42] Sheikh-ahmed JY. *Machining of Polymer Composites* 2013.
- [43] Ogedengbe TS, Okediji AP, Yussouf AA, Aderoba OA, Abiola OA, Alabi IO, et al. The Effects of Heat Generation on Cutting Tool and Machined Workpiece. *J Phys Conf Ser* 2019;1378. <https://doi.org/10.1088/1742-6596/1378/2/022012>.
- [44] Merino-Pérez J L, Hodzic A, Merson E, Ayvar-Soberanis S. On the temperatures developed in CFRP drilling using uncoated WC-Co tools Part II: Nanomechanical study of thermally aged CFRP composites. *Compos Struct* 2015;123:30–4.
- [45] Sekhar R, Singh TP. Mechanisms in turning of metal matrix composites: A review. *J Mater Res Technol* 2015;4:197–207. <https://doi.org/10.1016/j.jmrt.2014.10.013>.
- [46] AFNOR-Couple outil-matière : Domaine de fonctionnement des outils coupants. (NF E 66-520). 1994.
- [47] Takeyama, H. and N. Iijima, *Machinability of Glassfiber Reinforced Plastics and Application of Ultrasonic Machining*. *CIRP Annals - Manufacturing Technology*, 1988. 37(1): p. 93-96.
- [48] König, W. and P. Grass, *Quality definition and assessment in drilling of fibre reinforced thermosets*. *CIRP Annals-Manufacturing Technology*, 1989. 38(1): p. 119-124.
- [49] Giasin, K., *Machining Fibre Metal Laminates and Al2024-T3 aluminium alloy*. 2017, University of Sheffield.
- [50] Pramanik, A. and G. Littlefair, *Developments in Machining of Stacked Materials Made of CFRP and Titanium/Aluminum Alloys*. *Machining Science and Technology*, 2014. 18(4): p. 485-508.
- [51] Eneyew ED, Ramulu M. Experimental study of surface quality and damage when drilling unidirectional CFRP composites. *J Mater Res Technol* 2014;3:354–62. <https://doi.org/10.1016/j.jmrt.2014.10.003>.
- [52] Li MJ, Soo SL, Aspinwall DK, Pearson D, Leahy W. Influence of lay-up configuration and feed rate on surface integrity when drilling carbon fibre reinforced plastic (CFRP) composites. *Procedia CIRP* 2014;13:399–404. <https://doi.org/10.1016/j.procir.2014.04.068>.
- [53] Coromant, S., *Machining carbon fibre materials, in Sandvik coromant user's guide - composite solutions* 2010.
- [54] SenthilKumar, M., A. Prabukarthi, and V.J.P.e. Krishnaraj, *Study on tool wear and chip formation during drilling carbon fiber reinforced polymer (CFRP)/titanium alloy (Ti6Al4*

- V) stacks. 2013. 64: p. 582-592.
- [55] Yaşar, N., M. Boy, and M. Günay. The effect of drilling parameters for surface roughness in drilling of AA7075 alloy. in MATEC Web of Conferences. 2017. EDP Sciences.
- [56] Jawahir IS, Chip-forms, Chip breakability and Chip Control. CIRP Encyclopedia of Production Engineering, 2014: p.178-194.
- [57] Haddad M. Étude De L'Impact Des Défauts D'Usinage Des Structures Composites Par Détourage Sur Leur Comportement Mécanique 2013.
- [58] Vogel L. L'organisation de la prevention sur les lieux de travail. 1989.
- [59] Yoder T, Greene B, Porter A. Carbon Structure Hazard Control. 2015.
- [60] Cadorin, N. Zitoune, R. Seitier, P. Collombet, F. Analysis of damage mechanism and tool wear while drilling of 3D woven composite materials using internal and external cutting fluid. Journal of Composite Materials, 2015. Vol. 49 (22), p. 2687-2703.

Figures

Fig. 1. (a) Illustrations of lay-up sequence in each GFRP layer for GLARE 2B 11/10-0.4 laminates, (b) Different tools used in the drilling trials, (c) Glare specimen and Kistler dynamometer, (d) system of acquisition.

Fig. 2. (a) Mitutoyo SJ-500/P surface roughness instrument (b) the four points of roughness measurements (c) Mitutoyo three dimensional CMM device for cylindricity measurements.

Fig. 3. A typical thrust force and torque measurement during a drilling cycle (For tool T1, N= 3000 rpm, f=0.12 mm/rev).

Fig. 4. Evolution of thrust force (a) versus feed (b) versus spindle speed and evolution of torque (c) at constant spindle speed 3000 rpm (d) at constant feed 0.055 mm/rev.

Fig. 5. Specific cutting force associated (a) with feed for T1, T2 and T3, (b) associated with the spindle speed for T1, T2 and T3.

Fig. 7. Average surface roughness profile for a drilled hole in GLARE 2B

Fig. 6. R_a and R_t for T1 and T3 (a) versus feeds and (b) spindle speeds.

Fig. 8. R_z values measured at positions of 0° , 45° , 90° and 180° for T2 (a) at different feeds and (b) at different spindle speeds and for T3 (c) at different feeds and (d) at different spindle speeds.

Fig. 9. Average circularity error for tools T1, T2 and T3 versus (a) feeds and (b) spindle speeds.

Fig. 10. Cylindricity at 3 depths versus feed for (a) tool T1 (b) tool T2 (c) tool T3 and versus spindle speeds for (d) tool T1 (e) tool T2 (f) tool T3.

Fig. 11. Cylindricity for tools T1, T2 and T3 versus (a) feeds and (b) spindle speeds.

Fig. 12. Chips geometric characteristics of GLARE 2B for T1 and T2 versus spindle speeds and feeds.

Fig. 13. Variation of the number of particles measured for different cutting parameters with (a) tool T1 (b) tool T2 (c) tool T3.

Fig. 14. Variation of the number of particles measured versus (a) feeds (b) spindle speeds

Fig. 15. Variation of total particles masses present in 1 L air (a) at constant spindle speed (b) at constant feed and evolution of harmful particles mass (c) at constant spindle speed (d) at constant feed.

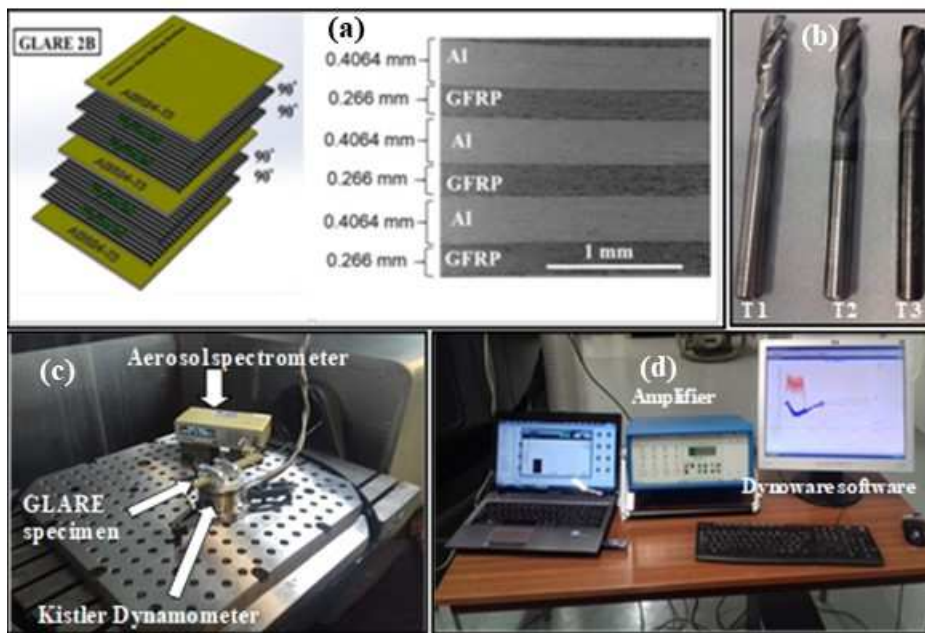


Fig. 1

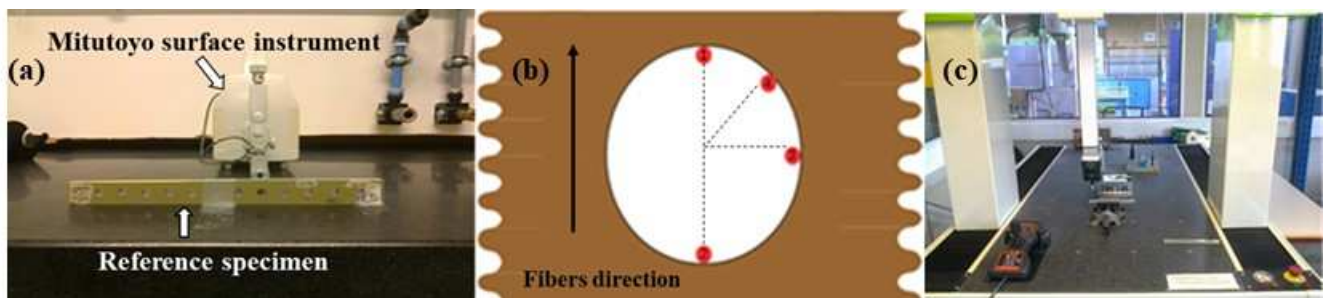


Fig. 2

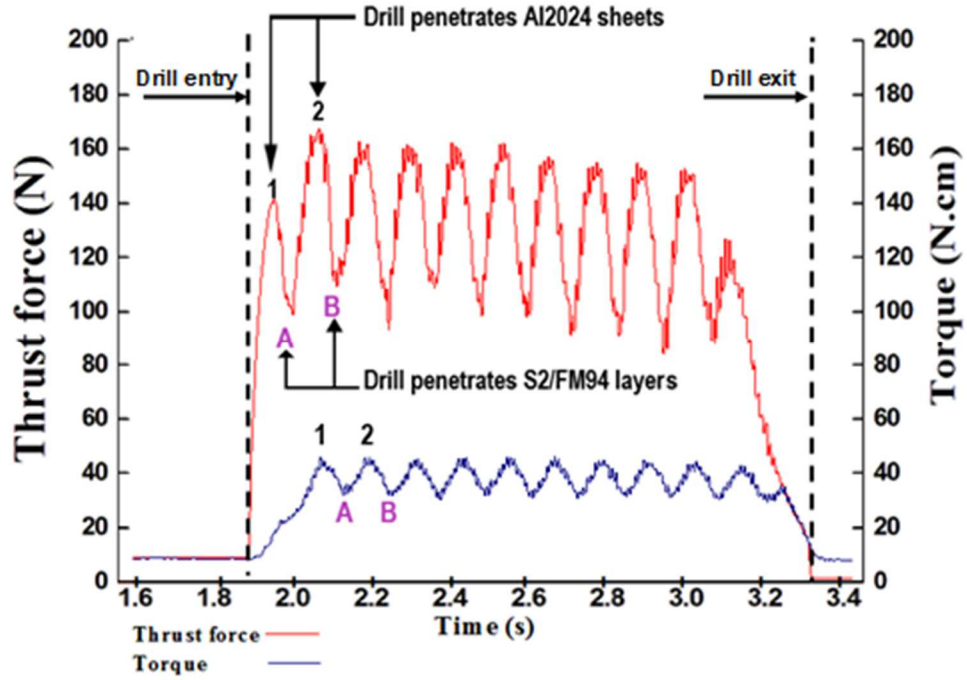


Fig. 3

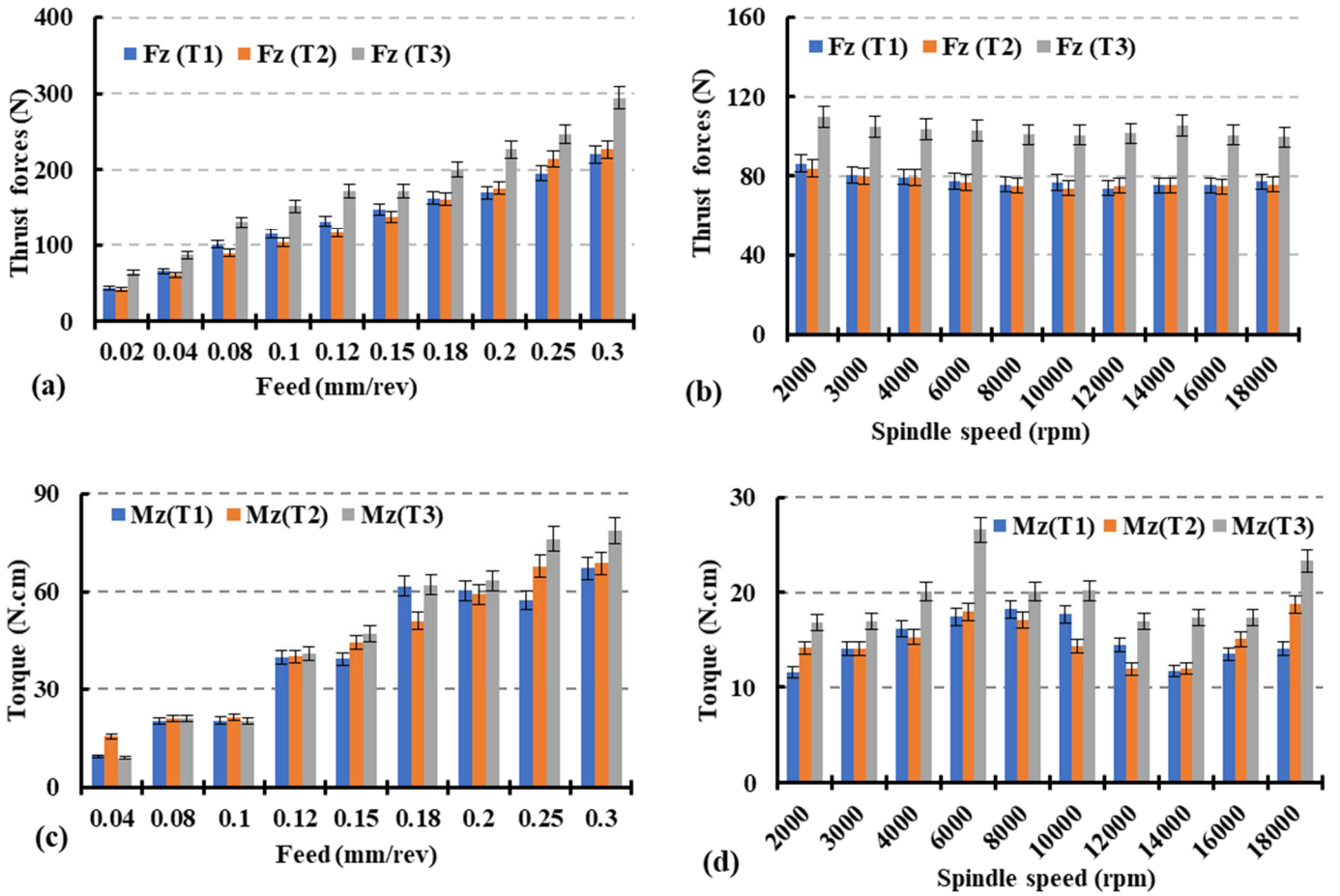


Fig. 4

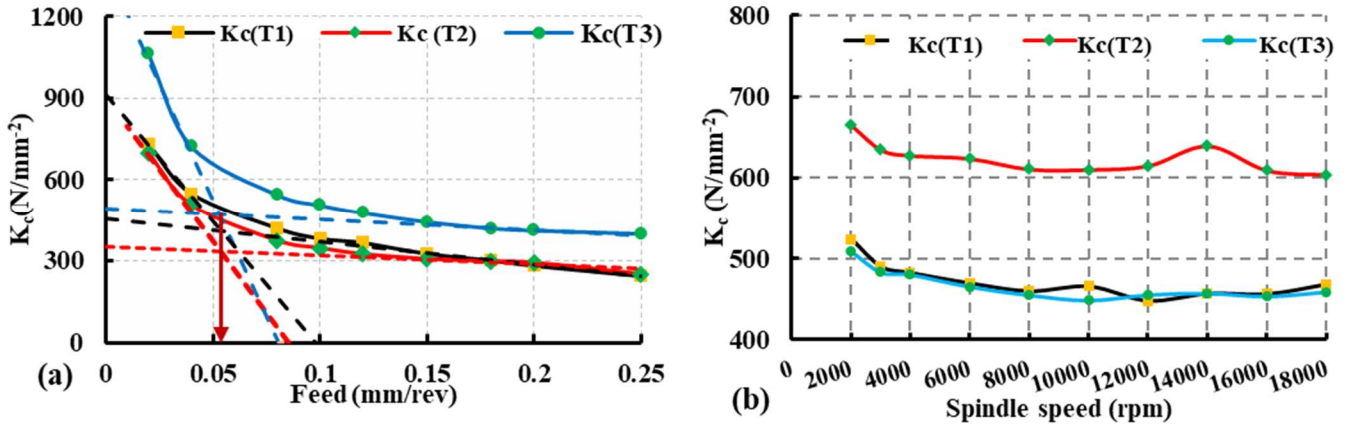


Fig. 5

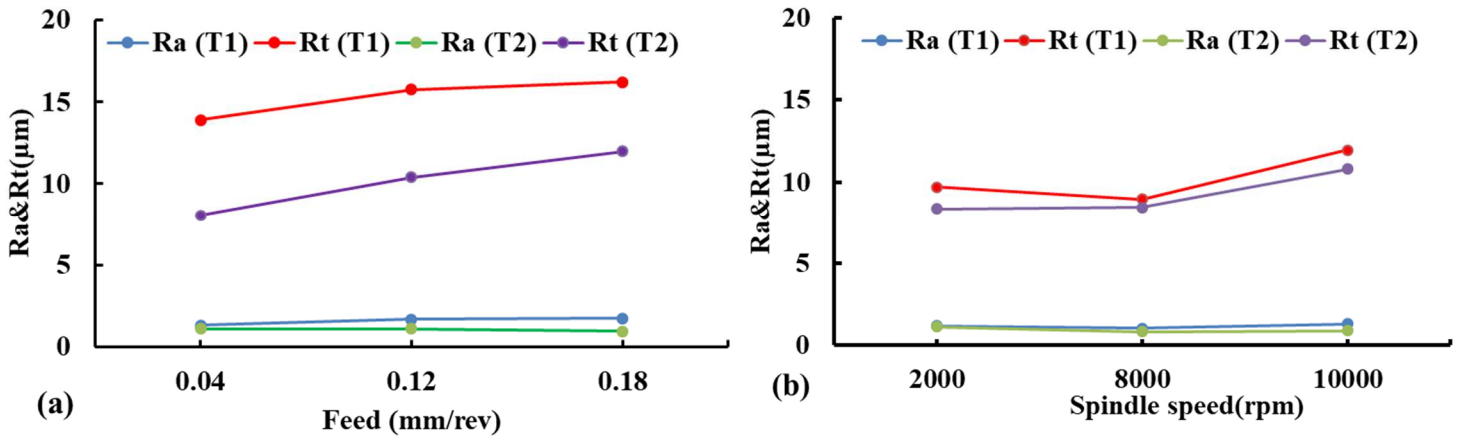


Fig. 6

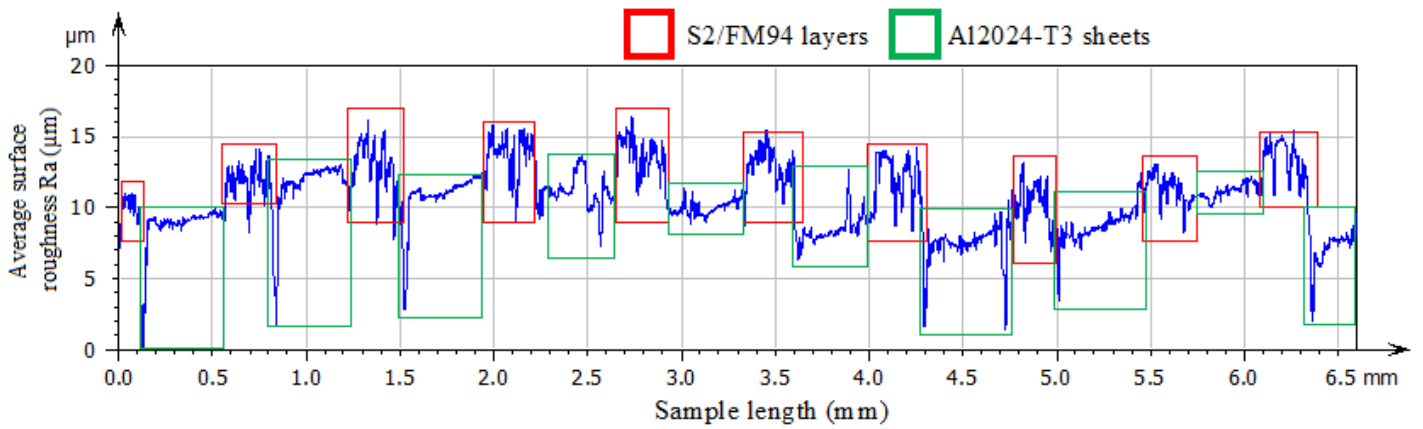


Fig. 7

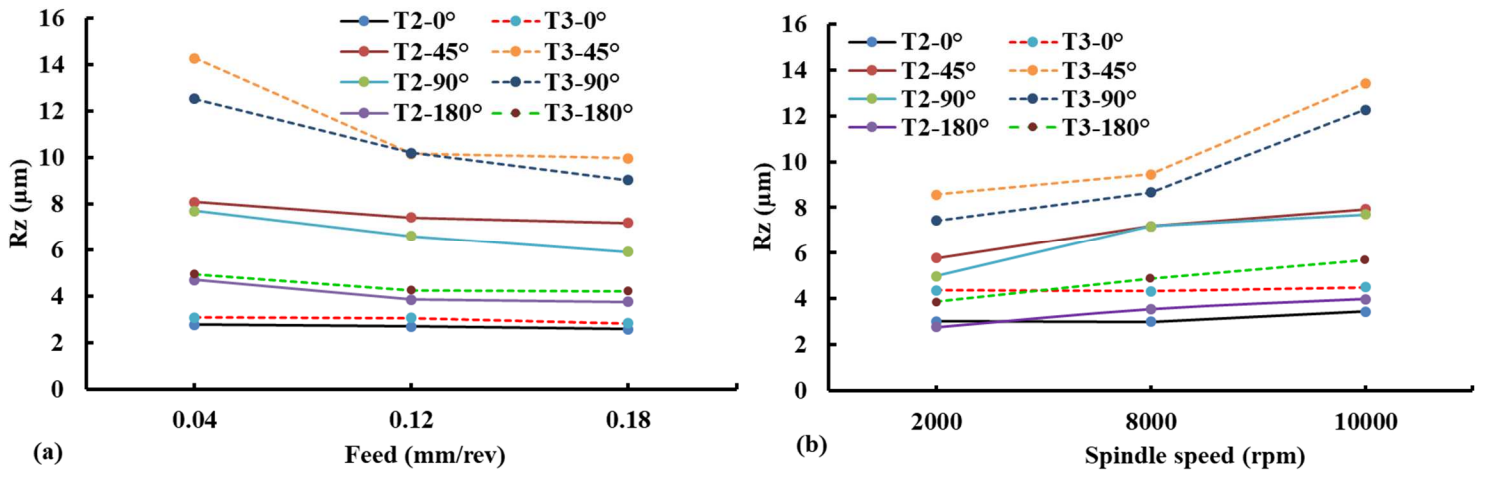


Fig. 8

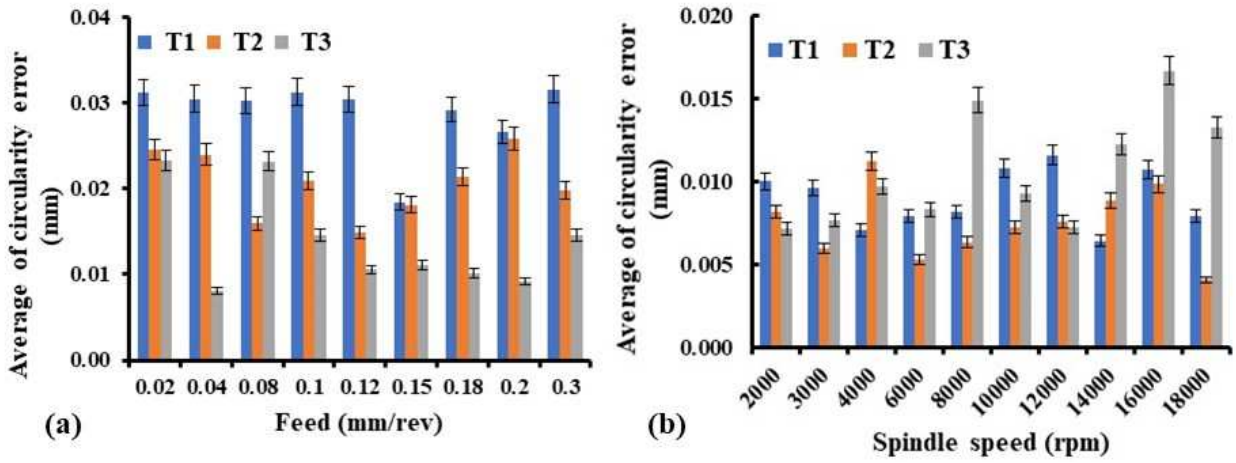


Fig. 9

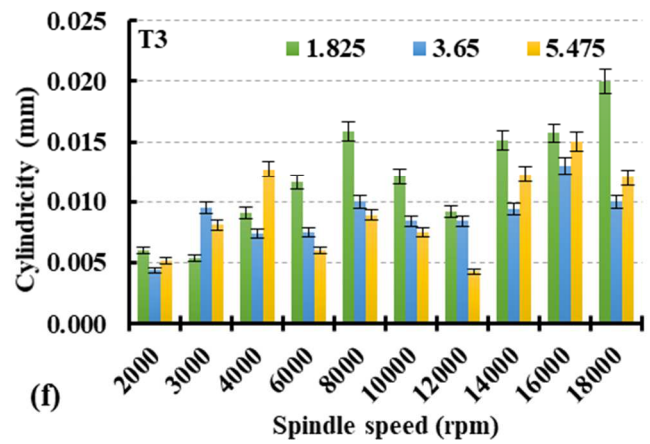
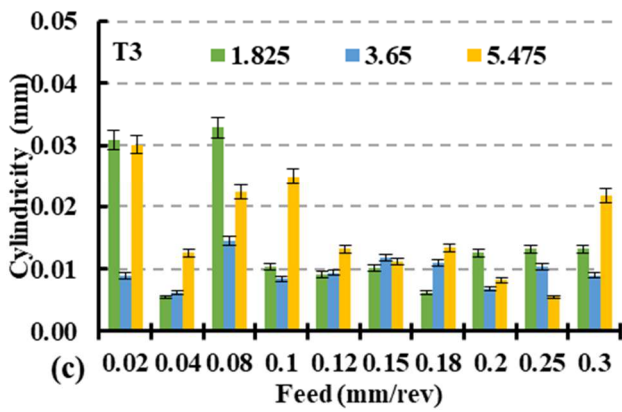
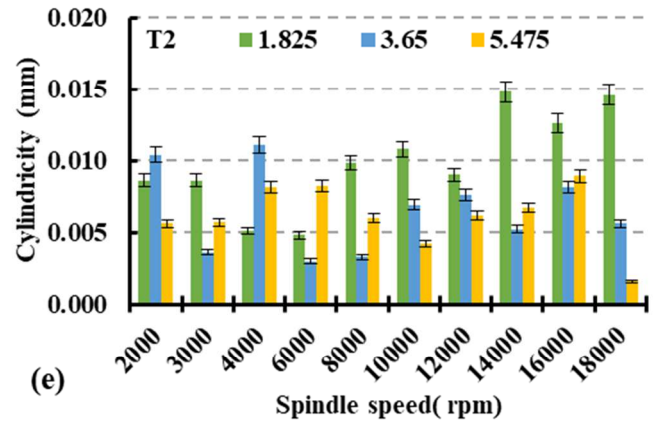
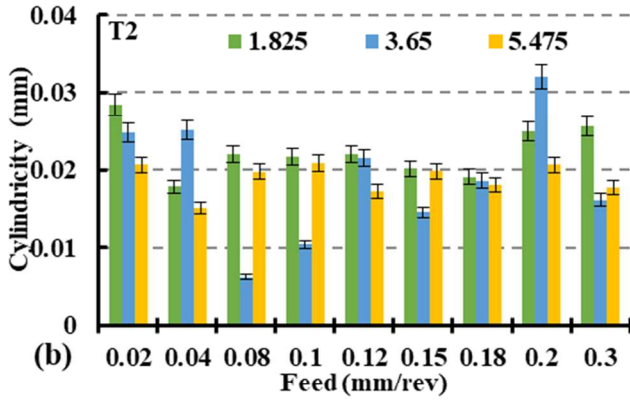
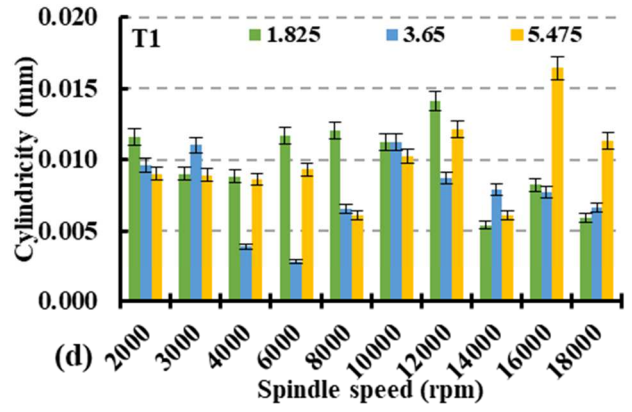
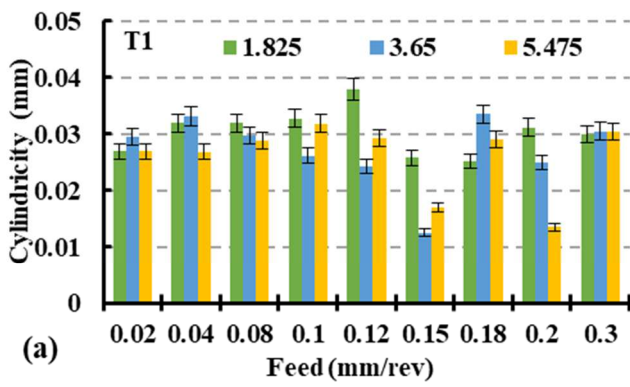


Fig. 10

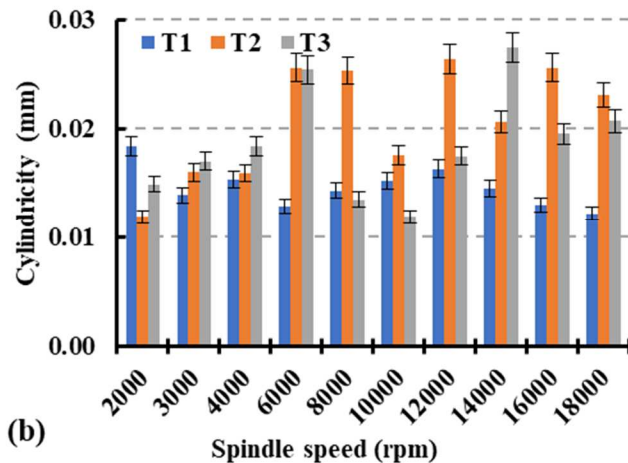
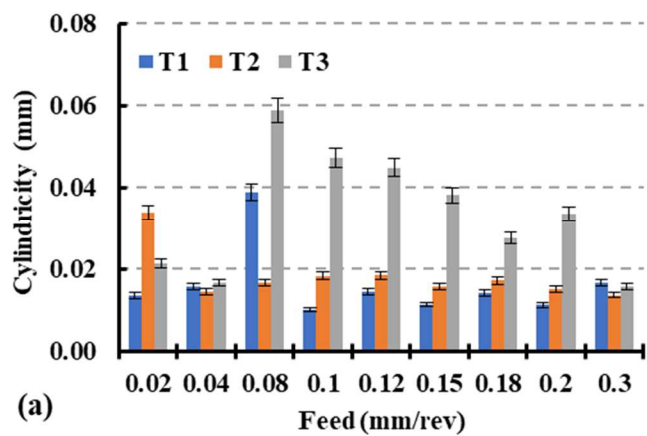


Fig. 11

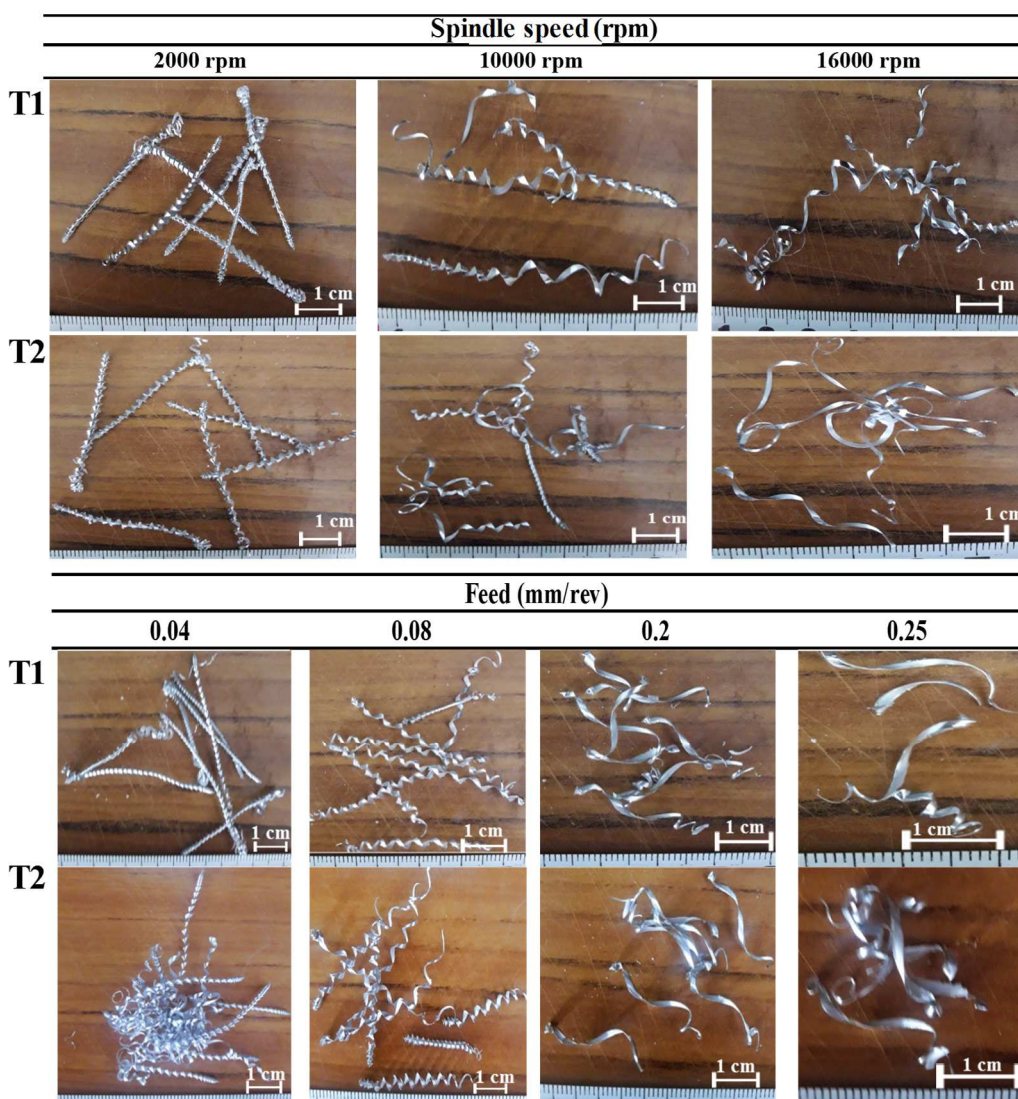


Fig. 12

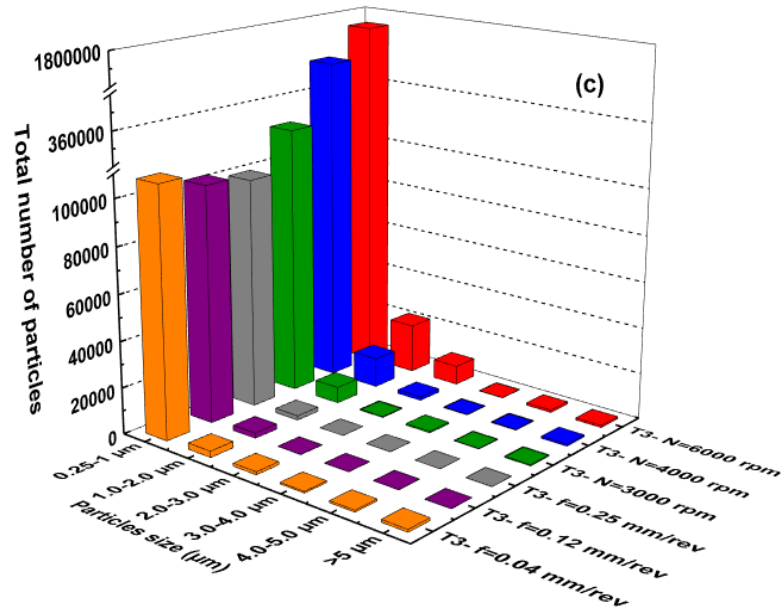
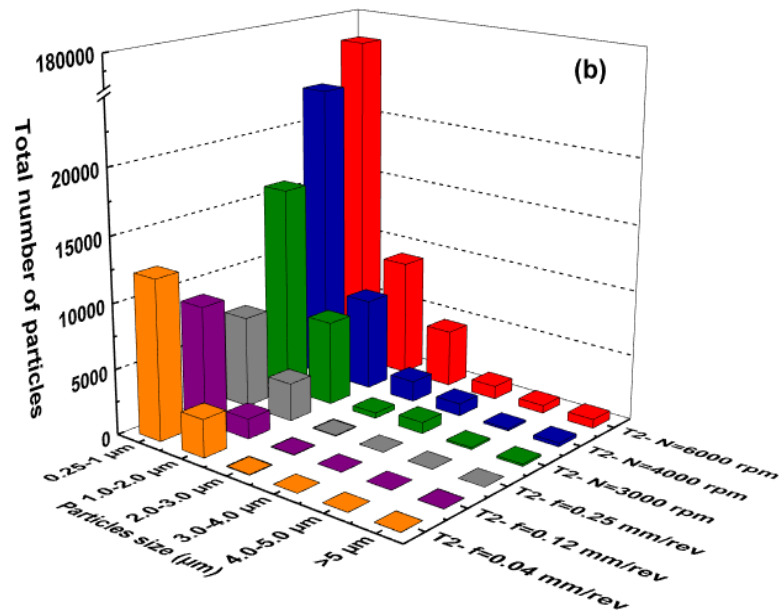
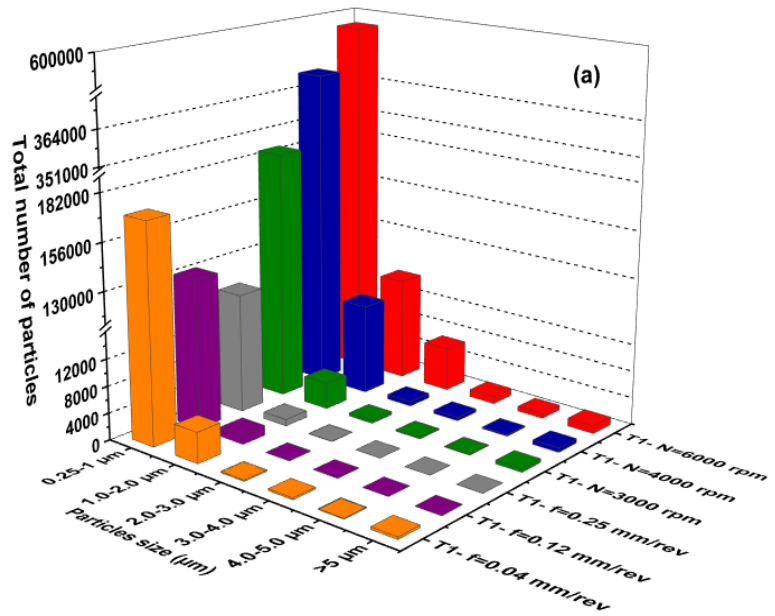


Fig. 13

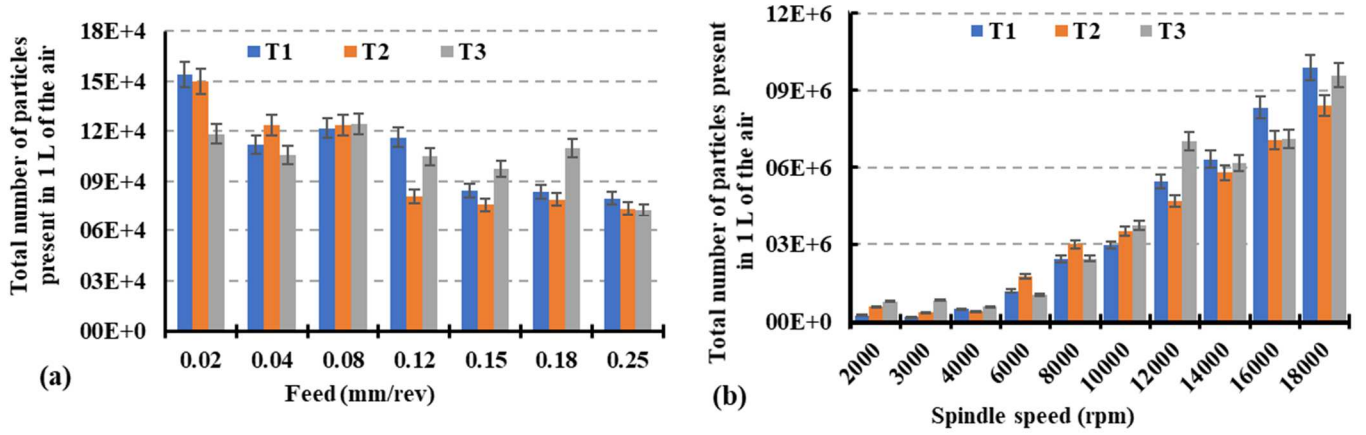


Fig. 14

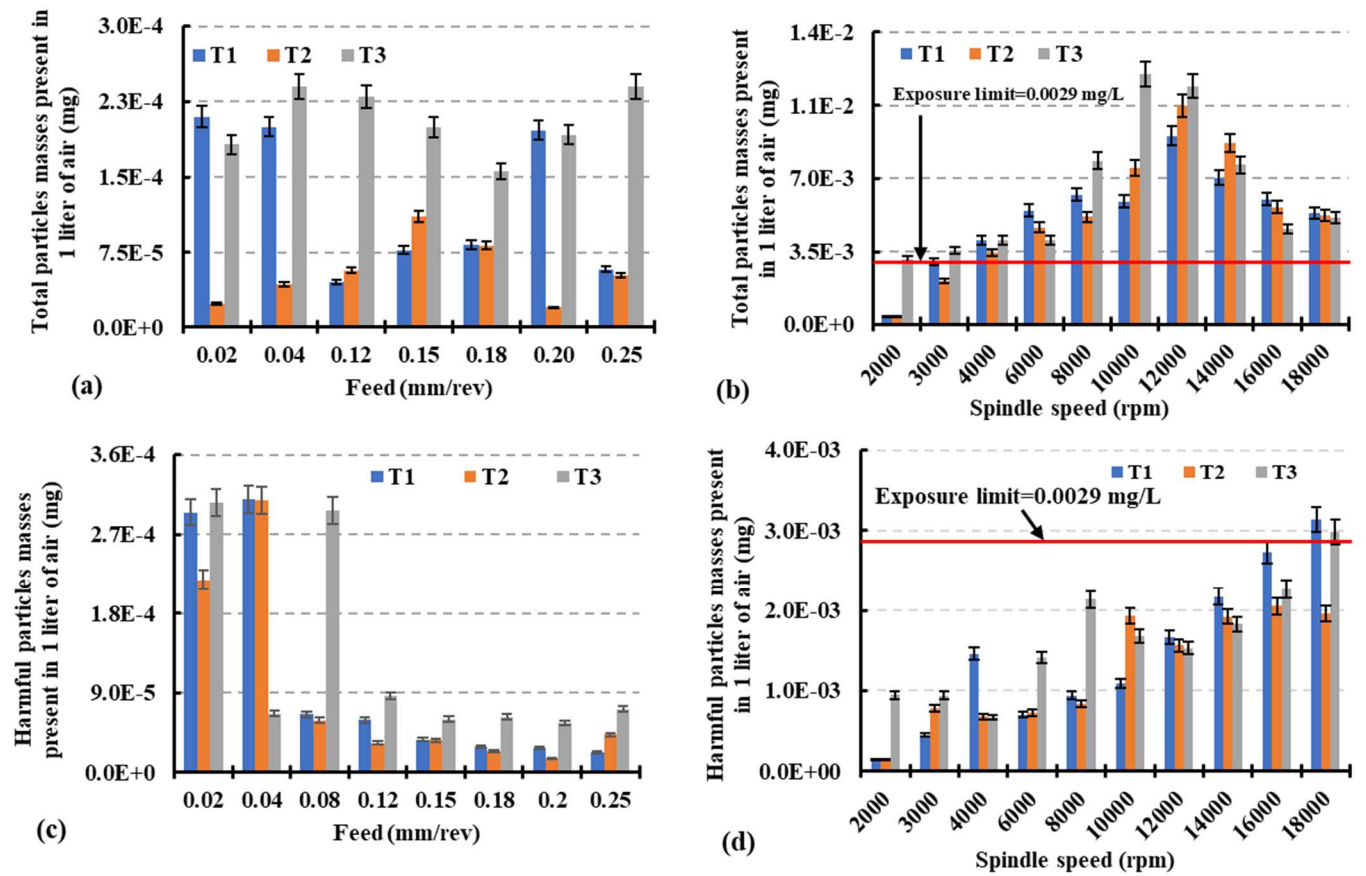


Fig. 15

Tables

Table 1 Mechanical properties of Al2024 alloy and S2/FM94 prepreg

Table 2 Properties of GLARE 2B 11/10-0.4

Table 3 Cutting tools specifications

Table 4 Drilling conditions used in experimental study

Table 5 Number of harmful particles for each range particle size

Table 1

Mechanical properties of Al2024 alloy and S2/FM94 prepreg

Mechanical property	Symbol	UD S2/FM94 epoxy prepreg	Al2024-T3
	E_{11}	54-55	72.2
Young modulus (GPa)	E_{22}	9.4-9.5	-
	E_{33}	9.4-9.5	-
	σ_{ult}	2640	455
Ultimate tensile strength (MPa)			
Ultimate strain (%)	ϵ_{ult}	4.7	19
Shear modulus (GPa)	G_{12}	5.55	27.6
	G_{23}	3	-
	G_{13}	5.55	-
	ν_{12}	0.33	0.33
Poisson's ration	ν_{23}	0.0575	-
	ν_{13}	0.33	-
Density(kg/m ³)	ρ	1980	
Thermal conductivity (W/m.K)	k	1.1-1.4	121

Table 2

Properties of GLARE 2B 11/10-0.4

Type of GLARE	GLARE 2B 11/10-0.4
Thickness of aluminum layer (mm)	0.4064 [Fig.1]
Thickness of S2 glass fiber layer (mm)	0.266 [Fig.1]
Total thickness (mm)	7.13
Metal volume fraction % (M.V.F)	62.69
Work-piece size (mm*mm)	205*100

Table 3

Cutting tools specifications

Label	T1	T2	T3
Tool material		Solid Carbide	
Carbide type		K20	
Carbide grade		DK 255F (92% WC, 8% Co)	
Surface finish	Uncoated	DLC (Diamond like carbon coating)	Cristall (Diamond coating)
Diameter (mm)		6	
Manufacturer		GUHRING®	

Table 4

Drilling conditions used in experimental study

Feed (mm/rev)	0.02, 0.04, 0.08, 0.1, 0.12, 0.15, 0.18, 0.25, 0.3
Spindle speed (rpm)	2000,3000, 4000, 6000, 8000, 10000, 12000, 14000, 16000, 18000

Table 5

Number of harmful particles for each range of particles size

$A = 0.994 * N_{[0.25-0.28]}$	Number of harmful particles sizing from 0.25 μm to 0.28 μm with: *0.994 is the percentage of harmful particles sizing from 0.25 μm to 0.28 μm . * $N_{[0.25-0.28]}$ is the number of total particles sizing from 0.25 μm to 0.28 μm .
$B = 0.99 * N_{[0.3-0.35]}$	Number of harmful particles sizing from 0.3 μm to 0.35 μm .
$C = 0.95 * N_{[0.4-0.45]}$	Number of harmful particles sizing from 0.4 μm to 0.45 μm .
$D = 0.9 * N_{[0.5-0.58]}$	Number of harmful particles sizing from 0.5 μm to 0.58 μm .
$E = 0.85 * N_{[0.65-0.7]}$	Number of harmful particles sizing from 0.65 μm to 0.7 μm .
$F = 0.8 * N_{[0.8-1]}$	Number of harmful particles sizing from 0.8 μm to 1 μm .
$G = 0.7 * N_{[1.3-1.6]}$	Number of harmful particles sizing from 1.3 μm to 1.6 μm .
$H = 0.6 * N_{[2-2.5]}$	Number of harmful particles sizing from 2 μm to 2.5 μm .
$I = 0.55 * N_{[3-3.5]}$	Number of harmful particles sizing from 3 μm to 3.5 μm .
$J = 0.5 * N_{[4-5]}$	Number of harmful particles sizing from 4 μm to 5 μm .
$K = 0.45 * N_{[6.5-7.5]}$	Number of harmful particles sizing from 6.5 μm to 7.5 μm .
$L = 0.4 * N_{[8.5-10]}$	Number of harmful particles sizing from 8.5 μm to 10 μm .
$M = 0.05 * N_{>10}$	Number of harmful particles sizing over 10 μm .